The Plant Cell, Vol. 32: 2216–2236, July 2020, www.plantcell.org © 2020 ASPB.

STRESS INDUCED FACTOR 2 Regulates Arabidopsis Stomatal Immunity through Phosphorylation of the Anion Channel SLAC1

Ching Chan,[a,b,1] Dario Panzeri,[a,1] Eiji Okuma,[c,2] Kadri Tõldsepp,[d,2] Ya-Yun Wang,[a,2] Guan-Yu Louh,[a] Tzu-Chuan Chin,[a] Yu-Hung Yeh,[a] Hung-Ling Yeh,[b] Shweta Yekondi,[a] You-Huei Huang,[a] Tai-Yuan Huang,[a] Tzyy-Jen Chiou,[b] Yoshiyuki Murata,[c] Hannes Kollist,[d] and Laurent Zimmerli[a,3]

[a] Department of Life Science and Institute of Plant Biology, National Taiwan University, Taipei 106, Taiwan
[b] Agricultural Biotechnology Research Center, Academia Sinica, Taipei 115, Taiwan
[c] Graduate School of Environmental and Life Science, Okayama University, Okayama 700-8530, Japan
[d] University of Tartu, Tartu 50411, Estonia

ORCID IDs: 0000-0003-1954-0747 (C.C.); 0000-0003-3058-7482 (D.P.); 0000-0003-3767-5717 (E.O.); 0000-0003-0418-0160 (K.T.); 0000-0002-3823-2136 (Y.-Y.W.); 0000-0002-5973-2455 (G.-Y.L.); 0000-0003-4597-8742 (T.-C.C.); 0000-0002-5520-3206 (Y.-H.Y.); 0000-0002-8764-6378 (H.-L.Y.); 0000-0003-1234-5324 (S.Y.); 0000-0001-9297-4942 (Y.-H.H.); 0000-0003-1280-4295 (T.-Y.H.); 0000-0001-5953-4144 (T.-J.C.); 0000-0002-7864-1903 (Y.M.); 0000-0002-6895-3583 (H.K.); 0000-0002-3119-6638 (L.Z.)

Upon recognition of microbes, pattern recognition receptors (PRRs) activate pattern-triggered immunity. FLAGELLIN SENSING2 (FLS2) and BRASSINOSTEROID INSENSITIVE1-ASSOCIATED KINASE1 (BAK1) form a typical PRR complex that senses bacteria. Here, we report that the kinase activity of the malectin-like receptor-like kinase STRESS INDUCED FACTOR 2 (SIF2) is critical for Arabidopsis (*Arabidopsis thaliana*) resistance to bacteria by regulating stomatal immunity. SIF2 physically associates with the FLS2-BAK1 PRR complex and interacts with and phosphorylates the guard cell SLOW ANION CHANNEL1 (SLAC1), which is necessary for abscisic acid (ABA)-mediated stomatal closure. SIF2 is also required for the activation of ABA-induced S-type anion currents in Arabidopsis protoplasts, and SIF2 is sufficient to activate SLAC1 anion channels in *Xenopus* oocytes. SIF2-mediated activation of SLAC1 depends on specific phosphorylation of Ser 65. This work reveals that SIF2 functions between the FLS2-BAK1 initial immunity receptor complex and the final actuator SLAC1 in stomatal immunity.

INTRODUCTION

Plants sense microbial pathogens at different stages of infection and proliferation in a multilayered system called innate immunity. Early detection of pathogens is performed by cell surface-localized pattern-recognition receptors (PRRs) that sense microbe-associated molecular patterns (MAMPs; Monaghan and Zipfel, 2012). MAMPs are usually conserved parts of microbial molecules, such as the lipopolysaccharide (LPS) envelope or peptidoglycans of Gram-negative bacteria, the eubacterial flagellin and the elongation factor EF, methylated bacterial DNA fragments, fungal cell-wall-derived chitins, glucans, and proteins (Girardin et al., 2002; Boller and Felix, 2009).

Following recognition of MAMPs, plants activate a set of adaptive responses called pattern-triggered immunity (PTI) responses (Tsuda and Katagiri, 2010; Huang and Zimmerli, 2014). During PTI, pathogen recognition rapidly triggers calcium influx into the cytoplasm and nucleus (Gust et al., 2007; Ranf et al., 2011), the production of reactive oxygen species (ROS) (Gómez-Gómez et al., 1999), and signaling via mitogen-activated protein kinases (MAP kinases; Zhang and Klessig, 1998; Nühse et al., 2000). These early PTI events subsequently activate WRKY transcription-factor-mediated transcriptional reprogramming as well as calmodulin binding proteins (Boller and Felix, 2009; Tena et al., 2011). Concomitant with transcriptional reprogramming, plants activating the PTI response produce the signaling hormones ethylene, jasmonic acid-isoleucine conjugate, and salicylic acid (SA; Dodds and Rathjen, 2010). Deposition of callose at the cell wall also occurs a few hours after PTI activation (Gómez-Gómez et al., 1999).

In Arabidopsis (*Arabidopsis thaliana*), several PRRs have been characterized, including FLAGELLIN SENSING2 (FLS2; Gómez-Gómez and Boller, 2000), which recognizes the bacterial MAMP flagellin. PRRs work in tightly regulated complexes comprising several other proteins, notably receptor-like kinases (RLKs), membrane-bound kinases, and phosphatases (Macho and Zipfel, 2014). In PRR complexes, transphosphorylation events are crucial for downstream signaling (Petutschnig et al., 2010; Schulze et al., 2010; Schwessinger et al., 2011). In this context, one of the best-characterized coreceptors is BRASSINOSTEROID INSENSITIVE1-ASSOCIATED KINASE1 (BAK1; Chinchilla et al., 2007; Wang et al., 2008; Schulze et al., 2010; Schwessinger et al., 2011). In addition to acting in PTI, BAK1 also functions in abscisic acid (ABA)-mediated guard cell regulation (Ha et al., 2016).

[1] These authors contributed equally to this work.
[2] These authors contributed equally to this work.
[3] Address correspondence to lozim4@gmail.com.
The author responsible for distribution of materials integral to the findings presented in this article in accordance with the policy described in the Instructions for Authors (www.plantcell.org) is: Laurent Zimmerli (lozim4@gmail.com).
www.plantcell.org/cgi/doi/10.1105/tpc.19.00578

IN A NUTSHELL

Background: Like humans, plants are regularly attacked by microbes such as fungi and bacteria. An easy way for bacteria to penetrate into plant leaf tissue is through pores known as stomata. Stomata are essential for normal processes such as gas exchange for photosynthesis and the maintenance of transpiration pull for re-distribution of water and minerals throughout the plant. One of the first lines of defense to block bacterial entry into leaves is to close stomata. To do this, plants first need to sense the presence of bacteria through sensor proteins that detect bacteria. These sensors are called immunity receptors. After immunity receptors detect bacteria, other proteins relay the defense signal to quickly initiate defense responses including closing stomata. Revealing how bacteria are detected and how the downstream defense signal works should facilitate the development of crops with increased resistance to bacteria.

Question: We wanted to explore how plants regulate stomatal opening and closure to balance normal growth and immunity against bacterial attack. We asked questions such as: what gene(s) is(are) the sensor (who)? What are the downstream mechanisms leading to bacterial resistance (how)?

Findings: Using the model plant Arabidopsis, we found that mutation of the gene *STRESS INDUCED FACTOR 2 (SIF2)* leads to reduced plant resistance to infection by bacteria, indicating that SIF2 is necessary for full bacterial resistance. Our investigation revealed that SIF2 mostly acts during stomatal immunity. SIF2 physically associates with a key immunity receptor complex. SIF2 protein has an intra-cellular kinase domain and during bacterial infection, this kinase domain mediates phosphorylation of the ion channel SLAC1 at position Serine65. Phosphorylation and activation of SLAC1 then leads to stomatal closure. SIF2 works at stomata to relay the defense signal from the bacterial sensor or immunity receptor complex, to a key downstream player, SLAC1, which induces stomatal closure to restrict bacterial entry into leaves.

Next steps: SIF2 belongs to the receptor-like kinase family. The *Arabidopsis thaliana* genome has more than 600 genes encoding receptor-like kinases. Next, we will decipher how they differ from each other: do they sense or modulate different signals? Do they function together as a supramolecular complex or alone?

PRR signaling can trigger stomatal closure leading to stomatal immunity as one aspect of PTI (Melotto et al., 2006; Singh and Zimmerli, 2013). Notably, the recognition of bacteria through the binding of MAMPs by PRRs in guard cells induces rapid stomatal closure (Zeng and He, 2010). One of the key regulators of stomatal aperture is the hormone ABA, which triggers several intracellular messengers and signaling cascades, which ultimately acts on ion channels that cause a change in guard cell osmotic pressure (Pei et al., 1997; Schroeder et al., 2001; Munemasa et al., 2015). Typically, the anion channel SLOW ANION CHANNEL1 (SLAC1) acts as a key component of osmotic pressure regulation of guard cells (Vahisalu et al., 2008; Geiger et al., 2009; Lee et al., 2009). Downstream of ABA perception, the type-2C protein phosphatases ABA INSENSITIVE1 (ABI1) and ABI2 are negative regulators of ABA signaling (Leung et al., 1997; Vlad et al., 2009), while OPEN STOMATA 1 (OST1) is a positive regulator of ABA-induced stomatal closure, acting upstream of ROS production (Mustilli et al., 2002).

RLKs are also directly involved in stomatal regulation. Notably, GUARD CELL HYDROGEN PEROXIDE-RESISTANT1 (GHR1) mediates stomatal closure upon drought stress and other signals through activation of SLAC1 (Hua et al., 2012; Sierla et al., 2018), and BAK1 is involved in ABA-mediated guard cell signaling as it interacts with, and phosphorylates, OST1 (Ha et al., 2016). For bacteria- and MAMP-induced stomatal closure in Arabidopsis, both ABA and SA synthesis and signaling pathways are necessary (Melotto et al., 2006; Zeng et al., 2010). In addition, an ABA-independent oxylipin pathway controls stomatal immunity through SLAC1 (Montillet et al., 2013). Importantly, flg22-induced stomatal closure requires a functional SLAC1 (Guzel Deger et al., 2015), GHR1 (Hua et al., 2012), and partially OST1, as *ost1-2* mutants are insensitive to low concentrations of flg22 but show wild-type sensitivities to higher doses (Montillet et al., 2013). Among the RLKs involved in stomatal regulation, LecRK-V.5 was identified as a repressor of stomatal immunity that likely acts upstream of ROS production (Desclos-Theveniau et al., 2012), and LecRK-VI.2 was shown to act as a positive regulator of PTI, including stomatal immunity (Singh et al., 2012; Singh and Zimmerli, 2013).

In order to identify novel players in Arabidopsis defenses, we followed a reverse genetic approach with genes induced by MAMPs or bacteria (Postel et al., 2010). A T-DNA insertion mutant in the malectin-like leucine-rich repeat receptor-like kinase gene At1g51850, known as *STRESS INDUCED FACTOR 2* (*SIF2*; Yuan et al., 2018), demonstrated increased sensitivity to bacteria and impaired stomatal closure upon *Pseudomonas syringae* pv *tomato* (*Pst*) DC3000 inoculation or after flg22 or ABA treatment. All the mutant phenotypes were rescued when *sif2-1* was complemented by a wild-type SIF2 protein, but not by a kinase-dead SIF2 variant. Biochemical analyses revealed that SIF2 physically associates with the PRRs FLS2/BAK1 and with the anion channel SLAC1 in a ligand-independent manner. SIF2 kinase activity was necessary for the transphosphorylation of SLAC1 N-terminal domain, suggesting a functional link between SIF2 and SLAC1. Patch-clamp analysis using Arabidopsis guard cell protoplasts showed that SIF2 is required for ABA-mediated S-type anion channel activity. We also identified putative phosphorylation sites on SLAC1. Together, these data clarify the role of SIF2 in the molecular signaling pathway leading to stomatal closure upon bacterial attack.

RESULTS

SIF2 Is Necessary for flg22-Mediated Stomatal Immunity

To identify novel components of the Arabidopsis PTI response, we undertook a reverse genetic approach with LRR-RLKs similar to

the positive regulator of PTI IMPAIRED OOMYCETE SUSCEPTIBILITY1 (IOS1; Yeh et al., 2016) and induced by MAMPs or bacteria (Postel et al., 2010). We identified a mutant line (SALK_068030) whose T-DNA insertion is in the gene At1g51850 (Supplemental Figure 1A), known as SIF2 (Yuan et al., 2018). Like IOS1 (Yeh et al., 2016), SIF2 is characterized by an extracellular malectin-like domain. In addition, SIF2 possesses one transmembrane and one RD kinase domain (Supplemental Figure 1B). In the *sif2-1* mutant, the T-DNA is inserted in the second exon at 437 base pairs downstream of the ATG start site (Supplemental Figure 1A). Furthermore, amplification of a region spanning the fifth and sixth exon downstream of the T-DNA insertion site by RT-qPCR revealed that *sif2-1* is a knockout mutant (Supplemental Figure 1C).

For complementation and overexpression studies, a Cauliflower mosaic virus 35S promoter-*SIF2* construct was introduced into homozygotic *sif2-1* mutant or Columbia (Col-0) wild type, respectively. Two lines homozygotic for each transformation were named complementation by overexpression 1 and 2 (CO1 and CO2) and overexpression 1 and 2 (OE1 and OE2). *SIF2* expression levels in CO1 or CO2 and OE1 or OE2 lines are shown in Supplemental Figures 1D and 1E, respectively. Furthermore, analysis of *SIF2* transcript levels in CO and OE lines showed that CO1 and CO2 lines harbored wild-type-like *SIF2* expression levels, while OE1 and OE2 lines demonstrated a clear upregulation of *SIF2* expression (Supplemental Figure 1F).

To evaluate the potential role of SIF2 in resistance to bacteria, the *sif2-1* mutant was dip-inoculated with virulent, hemibiotrophic bacteria *Pst* DC3000. The loss-of-function mutant *sif2-1* demonstrated stronger bacteria-mediated symptoms at 3 d after inoculation (DAI) and increased bacterial titers at 2 DAI when compared to wild-type controls (Figure 1A). To confirm that disruption of SIF2 is responsible for the observed susceptibility to bacteria, disease severity was evaluated in CO1 and CO2 after dip-inoculation with *Pst* DC3000. CO1 and CO2 lines demonstrated wild-type resistance to bacteria (Figure 1A), indicating that a functional SIF2 is necessary for resistance to *Pst* DC3000. Furthermore, OE1 and OE2 were more resistant to *Pst* DC3000 infection (Figure 1B).

Next, we used the necrotrophic fungal pathogen *Botrytis cinerea* to investigate whether SIF2 is critical for Arabidopsis resistance to another type of microbial pathogen. For that purpose, 5-week-old Arabidopsis were droplet-inoculated with *B. cinerea*, and lesion perimeters were evaluated 3 d later. Lesion sizes were similar to wild type in *sif2-1*, CO1, and CO2 plants, suggesting that SIF2 does not play a critical role in Arabidopsis resistance to *B. cinerea* (Supplemental Figure 2). Taken together, these data suggest that SIF2 is necessary for full resistance to *Pst* DC3000 bacteria, but not for resistance to *B. cinerea* fungi.

Although *sif2-1* showed increased susceptibility to *Pst* DC3000 after surface inoculation (Figure 1A), no difference in disease susceptibility was observed after infiltration inoculation (Supplemental Figures 3A and 3B). Infiltration inoculation bypasses the first defense barrier, notably stomatal closure, which restricts bacteria entry into leaves (Melotto et al., 2006; Zeng and He, 2010). Typically, *Pst* DC3000 bacteria induce stomatal closure within 1 to 1.5 h postinoculation. However, virulent bacteria such as *Pst* DC3000 secrete the chemical effector coronatine, which induces reopening of stomata (Melotto et al., 2006; Zeng and He, 2010). To test whether SIF2 is critical for stomatal immunity, epidermal peels of Col-0 wild type, *sif2-1*, CO1, and CO2 plants were floated in a solution containing 10^8 cfu/mL *Pst* DC3000 for 1 and 3 h. As expected (Melotto et al., 2006), rapid stomatal closure was observed in Col-0 wild type after *Pst* DC3000 inoculation, while reopening occurred at 3 h postinoculation (hpi; Figure 1C). Stomatal closure was not observed in the *sif2-1* mutant, while the complementation lines CO1 and CO2 demonstrated wild-type stomatal closure at 1 hpi (Figure 1C). Lines overexpressing *SIF2* showed stomatal closure at 1 hpi and partial constitutive stomatal closure (Supplemental Figure 4A). Importantly, the stomatal length and width of OE lines were similar to those of wild-type Col-0 stomata (Supplemental Figure 4B), suggesting that constitutive stomatal closure in OE lines is not a consequence of smaller stomatal size. In addition, stomata of *sif2-1* demonstrated partial insensitivity to treatment with the MAMP flg22 (Figure 1D). To determine SIF2 specificity toward MAMPs, epidermal peels of the *sif2-1* mutant were exposed to 50 μg/mL of the fungal MAMP chitin (Lee et al., 1999) or to 100 ng/mL LPSs derived from outer membranes of Gram-negative bacteria (Desclos-Theveniau et al., 2012). The *sif2-1* mutant demonstrated a wild-type stomatal response (Supplemental Figure 5), suggesting that SIF2 is not critical for chitin- and LPS-induced stomatal closure. Together, these data suggest that SIF2 is required for stomatal movement and positively regulates flg22-mediated stomatal immunity.

To evaluate whether SIF2 plays a role in early apoplastic PTI, MPK3 and MPK6 phosphorylation levels (Nühse et al., 2000) and ROS production were evaluated. The mutant *sif2-1*, CO, and OE lines showed wild-type activation levels of MPK3/MPK6 and ROS production (Supplemental Figures 6A to 6D). To test whether SIF2 is important for late PTI responses, we analyzed the up-regulation of PTI-responsive genes *FLG22-INDUCED RECEPTOR-LIKE 1* (*FRK1*) and *CYP81F2* cytochrome P450 (Xiao et al., 2007; Boudsocq et al., 2010) and callose deposition (Gómez-Gómez et al., 1999). Up-regulation of these two PTI marker genes was at wild-type levels in the *sif2-1* mutant, CO, and OE lines (Supplemental Figures 7A to 7D). By contrast, callose deposition was at lower levels in the *sif2-1* mutant (Supplemental Figure 7E), and OE lines showed significantly more callose deposition than wild-type controls (Supplemental Figure 7F). Collectively, these results indicate that SIF2 does not play a critical role in early apoplastic PTI but is important for some aspects, notably callose deposition, during the late apoplastic PTI response.

SIF2 Is Required for ABA-Dependent Guard Cell Responses

We showed that SIF2 is critical for full activation of Arabidopsis stomatal immunity. Stomatal immunity is known to be ABA and SA dependent (Melotto et al., 2006). To decipher the role of SIF2 in stomatal closure, we analyzed stomatal responses of *sif2-1* to ABA and SA treatment. Similar to flg22 treatment (Figure 1D), the *sif2-1* mutant largely showed a defective ABA-mediated stomatal closure, while stomata of wild-type Col-0 and the two complementation lines CO1 and CO2 were significantly more closed (Figure 1E). However, the *sif2-1* mutant demonstrated wild-type stomatal closure after SA treatment (Supplemental Figure 8).

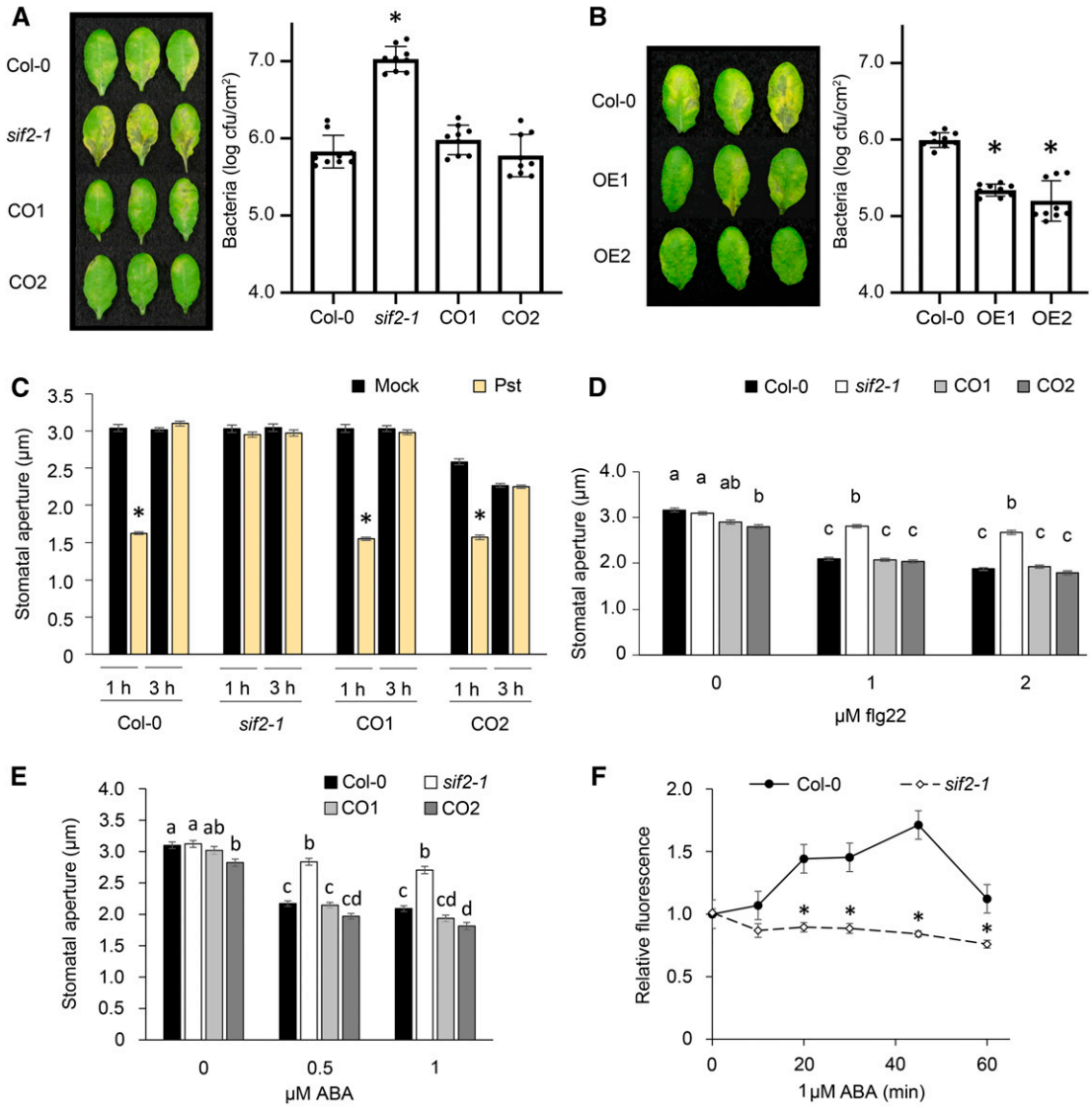

Figure 1. SIF2 Is Necessary for Full Stomatal Immunity.

(A) The *sif2-1* mutant is hyper-susceptible to *Pst* DC3000. Five-week-old plants were dip-inoculated in 10^6 cfu/mL *Pst* DC3000 for 15 min. Symptoms and titers were evaluated at respectively 3 and 2 DAI. Values represent average ± SEM from three independent experiments, each with three plants ($n = 9$). Asterisks indicate significant differences from the Col-0 wild type (WT) determined by a paired two-tailed Student's *t* test ($P < 0.05$).

(B) *SIF2* OE lines are more resistant to *Pst* DC3000. Plants were inoculated, and disease indexes were evaluated as in **(A)** in Col-0, OE1, and OE2 lines. Statistical analyses as in **(A)**.

(C) Stomatal closure upon *Pst* DC3000 inoculation. Epidermal peels of 5-week-old plants were floated in a suspension of 10^8 cfu/mL *Pst* DC3000 in 10 mM $MgSO_4$. Values represent average ± SEM from three independent experiments, each consisting of at least 50 stomata from three plants (9 plants, $n \geq 150$). Asterisks indicate significant differences from the mock as determined by a paired two-tailed Student's *t* test ($P < 0.001$).

(D) Stomatal closure upon flg22 treatment. Epidermal peels were floated in stomata buffer with flg22 at the indicated concentration. Stomatal openings were evaluated after 1 h. Values represent average ± SEM from three independent experiments, each consisting of at least 50 stomata from three plants (9 plants, $n \geq 150$). Letters represent significant difference ($P < 0.01$) when analyzed by one-way ANOVA with post-hoc Tukey HSD.

(E) Stomatal closure upon ABA treatment. Epidermal peels of 5-week-old plants were floated in stomatal buffer supplemented with ABA at the indicated concentrations. Stomatal openings were evaluated after 1 hour. Statistical analyses as in **(C)**.

(F) ROS accumulation in guard cells. Epidermal peels were stained with 50 µM H2DCFDA. ABA was then added to a final concentration of 1 µM, and H2DCFDA fluorescence was imaged at the indicated time points. Values represent average ± SEM from three independent experiments, each consisting of at least 50 stomata of three plants (9 plants, $n \geq 150$). Asterisks indicate significant differences from respective Col wild type determined with a Student's *t* test ($P < 0.001$).

To further evaluate the role of SIF2 in the ABA-dependent signaling in guard cells, epidermal peels of *sif2-1* and Col-0 wild type were exposed to ABA, and ROS accumulation in guard cells was observed with the fluorescent dye 2′,7′-dichlorodihydrofluorescein diacetate (H2DCFDA; Lee et al., 1999; Pei et al., 2000). In a time course study, accumulation of ROS after ABA treatment was significantly reduced in the *sif2-1* mutant (Figure 1F). However, direct application of ROS closed *sif2-1* stomata at a wild-type level (Supplemental Figure 9). Taken together, these data suggest that SIF2 is necessary for ABA-mediated stomatal closure, but not for closure of stomata in response to SA treatment.

The SIF2 Inactive Kinase Fails to Complement the *sif2-1* Loss-of-Function Mutant

As a member of the Arabidopsis LRR-RLKs, SIF2 possesses a putative cytoplasmic kinase domain (Hok et al., 2011), which shows a high degree of similarity to its homolog IOS1 and to BAK1 (Figure 2A). Notably, all the key residues known to be important for kinase activity are conserved in SIF2 (Figure 2A; Hanks and Hunter, 1995; Johnson et al., 1996). The FLS2 kinase domain is the most divergent of the four, and in contrast to the others is a non-RD kinase (Figure 2A; Johnson et al., 1996; Dardick and Ronald, 2006). SIF2 exhibited auto-phosphorylation activity when expressed in *Escherichia coli* (Figure 2B). By contrast, an inactive SIF2 kinase version produced by mutating the Asp residue of the arginine-aspartate (RD) motif, which is known to be critical for kinase activity (Johnson et al., 1996), into an Asn (D683N; Knighton et al., 1991; Schwessinger et al., 2011; Yeh et al., 2016) did not demonstrate autophosphorylation activity (Figure 2B). Similar to BAK1, a mobility shift on SDS-PAGE was observed between the active and inactive kinase (Figure 2B; Schwessinger et al., 2011). These observations suggest that the SIF2 kinase domain is active.

In order to investigate whether the SIF2 kinase activity is required for its function in planta, two *sif2-1* complementation lines named KD1 and KD2 for Kinase inactive/Dead form were generated by overexpression of the dead kinase SIF2 (D683N). Transgene expression was analyzed by reverse transcription quantitative PCR (RT-qPCR; Supplemental Figure 1F). KD1 and KD2 could not complement the increased *Pst* DC3000 susceptibility phenotype of *sif2-1*, but the CO1 did (Figure 2C). In addition, stomatal closure in KD1 and KD2 lines was not observed at 1 hpi with *Pst* DC3000 bacteria, while stomatal closure in the CO1 line was at wild type levels (Figure 2D). Similar to the *sif2-1* mutant, stomata of KD1 and KD2 lines did not close in response to flg22 or ABA treatments (Figures 2E and 2F). Together, these results indicate that the Asp residue of the RD motif (D683) of SIF2 is required for full resistance to bacteria and stomatal immunity activation. These observations also suggest that SIF2 kinase activity is essential for its function in defense.

SIF2 Is a Plasma Membrane-Localized Protein

SIF2 possesses a transmembrane domain (Supplemental Figure 1B) and is thus predicted to be plasma membrane localized. To analyze the subcellular localization of SIF2, we evaluated the GFP signal from the SIF2 overexpression line OE2 before and after plasmolysis, which revealed plasma membrane localization, notably in guard cells (Figure 3A). Transient expression of a PIP2-mCherry fusion protein that is known to be membrane localized (Li et al., 2011) driven by the Cauliflower mosaic virus 35S promoter in OE2 mesophyll protoplasts revealed colocalization of PIP2-mCherry and SIF2-GFP on the plasma membrane (Figure 3B). These observations suggest that like the PRRs FLS2, BAK1 (Robatzek et al., 2006; Häweker et al., 2010), and IOS1 (Yeh et al., 2016), SIF2 is localized at the plasma membrane.

We then investigated the localization of endogenous *SIF2* expression with a GUS reporter, driven by the *SIF2* promoter. We found distinct staining in guard cells, and this staining was further induced upon flg22 and *Pst* DC3000 elicitation (Figure 3C). This pattern suggests a specific role for SIF2 in the stomata. However, we do not rule out the possibility that basal expression of SIF2 in mesophyll cells (Winter et al., 2007) plays addition functions in other tissues, for example in mediating callose deposition.

SIF2 Forms a Protein Complex with FLS2 and BAK1

Since SIF2 modulates some aspects of the flg22-mediated PTI response and, like FLS2 and BAK1 (Robatzek et al., 2006; Häweker et al., 2010), is localized at the plasma membrane, we next asked whether SIF2 associates with FLS2 and BAK1. Toward this goal, we performed coimmunoprecipitation (CoIP) experiments using transgenic lines overexpressing SIF2-GFP. SIF2-GFP was immunoprecipitated with anti-GFP magnetic beads and analyzed for the presence of endogenous BAK1 and FLS2 using anti-BAK1 and anti-FLS2 immunoblotting. As a negative control, anti-GFP magnetic beads were incubated with protein extracts of untransformed Col-0 and transgenic plants expressing the low temperature and salt-responsive protein 6B (LTI6B/RCI2B) fused to GFP, which is known to localize at the plasma membrane (Cutler et al., 2000) and is usually used for such studies (Cutler et al., 2000; Kadota et al., 2014). Signals for FLS2 and BAK1 upon LTI6B-GFP immunoprecipitation were largely weaker than those observed upon SIF2-GFP immunoprecipitation (Figure 4A). In addition, no signals for FLS2 and BAK1 were detected for untransformed Col-0 (Figure 4A), suggesting that FLS2 and BAK1 do not non-specifically bind to anti-GFP magnetic beads, nor do they interact with GFP itself at the plasma membrane. By contrast, we could detect a clear association of SIF2-GFP with native FLS2 and BAK1 (Figure 4A). Treatment with flg22 did not affect significantly or reproducibly the associations of SIF2-GFP with FLS2 and BAK1 (Figure 4A). Interactions between SIF2 and FLS2, and BAK1 independently of flg22 treatment were also observed after CoIP experiments performed with a strong ultra-centrifugation step (Supplemental Figure 10; Rutter et al., 2017).

The bimolecular fluorescence complementation (BiFC) technique with Arabidopsis protoplasts was used to double confirm the interactions (Walter et al., 2004; Lee and Gelvin, 2014). To evaluate whether our experimental conditions were appropriate, we first analyzed the interaction between BAK1 and FLS2 that is known to occur only after flg22 elicitation (Chinchilla et al., 2007; Heese et al., 2007). As expected, YFP fluorescence was only detected in flg22-treated protoplasts (Figure 4B). By contrast, YFP fluorescence was observed before and after treatment with flg22

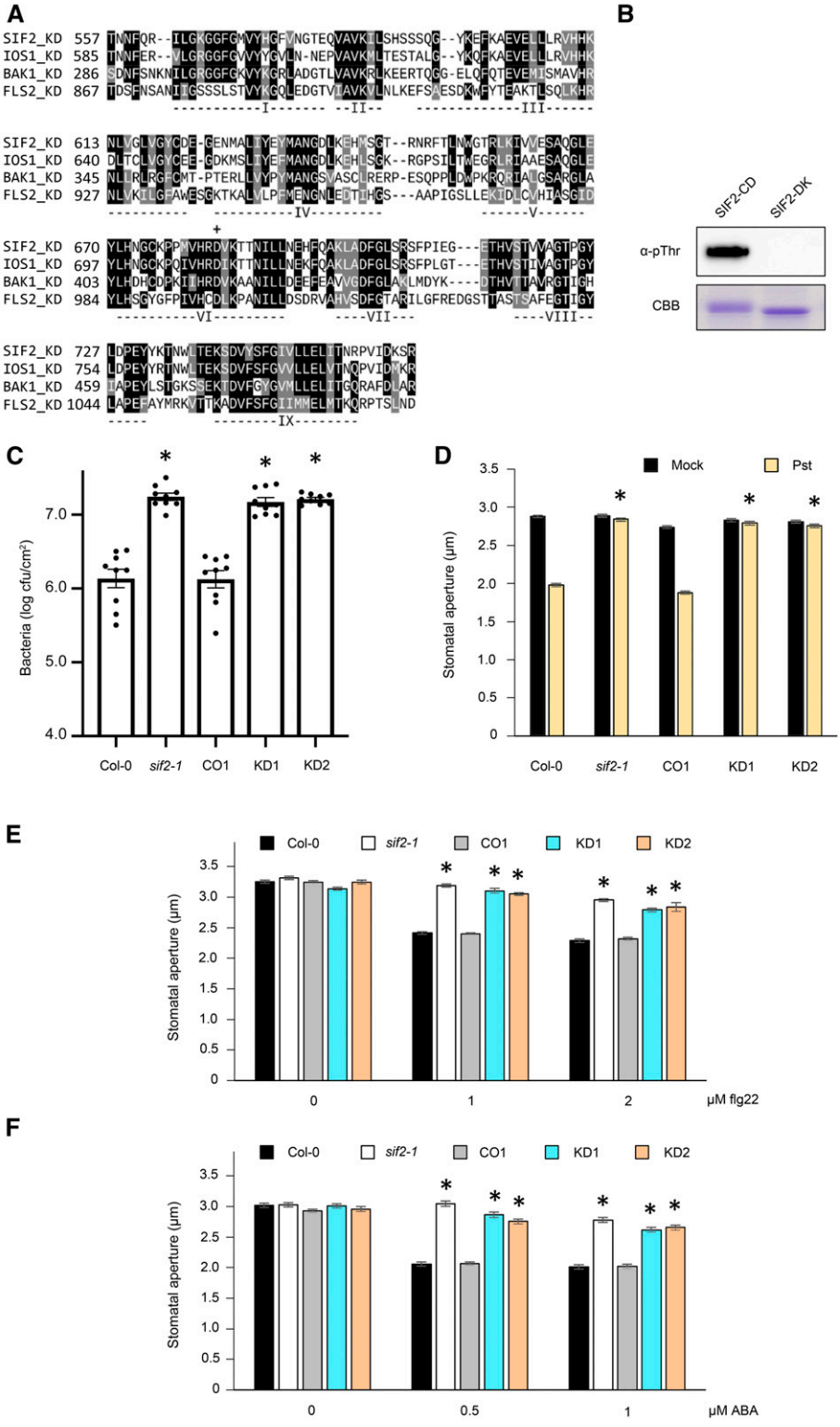

Figure 2. SIF2 Kinase Activity Is Essential for SIF2 Function.

(A) SIF2 harbors the typical LRR-RLK conserved domain (I to IX) and RD kinase domain (D683 asterisk).

when FLS2-YFP^N was cotransfected with SIF2-YFP^C (Figure 4B), suggesting that SIF2 interacts with FLS2 independently of flg22 elicitation. SIF2 association specificity was evaluated by testing SIF2 interaction with the membrane-localized LTI6B. No YFP signal was detected when LTI6B-YFP^N was cotransfected with SIF2-YFP^C (Figure 4B), suggesting that SIF2 does not interact with LTI6B. Importantly, LTI6B dimerization was observed indicating that the LTI6B constructs used were functional (Figure 4B). This observation illustrates the specificity of the SIF2-FLS2 interaction. In addition, a quantification of the fluorescence intensities of the 50 brightest protoplasts in each condition leads to the same conclusions (Figure 4C). Together, these data suggest that SIF2 interacts with the PRR FLS2 in a ligand-independent manner.

We also asked whether SIF2 interacts with BAK1, the coreceptor of FLS2 (Chinchilla et al., 2007; Heese et al., 2007; Sun et al., 2013). Toward this goal, BAK1-YFP^N was cotransfected with SIF2-YFP^C, and a positive signal was observed independently of flg22 elicitation (Figures 4B and 4C), suggesting that SIF2 also interacts with BAK1 in a ligand-independent manner. Taken together, in planta CoIP and protoplast BiFC analyses suggest association of SIF2 with FLS2 and BAK1 independently of flg22 treatment.

SIF2 Interacts with the Guard Cell Anion Channel SLAC1

The guard cell anion channel SLAC1 regulates both ABA- and flagellin-induced stomatal closure (Lee et al., 1999; Geiger et al., 2009; Vahisalu et al., 2010; Guzel Deger et al., 2015) and SIF2 is necessary for flg22- and ABA-mediated stomatal closure (Figures 1D and 1E). We thus asked whether SIF2 associates with SLAC1 using the CoIP approach in Arabidopsis protoplasts by transient coexpression of SIF2-HA$_3$ and SLAC1-GFP. A construct with GFP only was used as a negative control. After immunoprecipitation with GFP-Trap beads, we probed for SIF2-HA$_3$ by anti-HA immunoblotting and observed no signals with the GFP-only construct (Figure 5A). By contrast, positive association was detected for the combination of SIF2 and SLAC1 (Figure 5A). Using similar CoIP with a strong ultra-centrifugation step also revealed association between SIF2 and SLAC1 (Supplemental Figure 11). As observed for the LRR-RLK GHR1, a regulator of ABA-mediated stomatal closure (Hua et al., 2012), our CoIP data suggest association of SIF2 with the guard cell anion channel SLAC1.

The interaction between SIF2 and SLAC1 was further evaluated by BiFC analysis. Toward this goal, SIF2-YFP^N was cotransfected with SLAC1-YFP^C in Arabidopsis protoplasts. An increase in the fluorescent signal was observed independently of flg22 treatment (Figure 5B and 5C), suggesting interaction between SIF2 and SLAC1. LTI6B-YFP^N was used as a negative control to confirm that SLAC1-YFP^C specifically interacts with SIF2 when analyzed by BiFC (Figures 5B and 5C). Like SIF2, the malectin-like IOS1 interacts with FLS2 and BAK1 (Yeh et al., 2016). We thus asked whether IOS1 also plays a role in stomatal immunity through interaction with SLAC1. IOS1 did not show constitutive interaction with SLAC1 when analyzed by CoIP and BiFC (Supplemental Figures 11 and 12). This observation is not surprising, as IOS1 has only a marginal role in stomatal immunity (Yeh et al., 2016).

SIF2 Phosphorylates the SLAC1 N-Terminal Domain In Vitro

To test whether SIF2 can directly regulate the activation of SLAC1, a transphosphorylation assay was performed between purified SIF2 and SLAC1 fragments. The cytoplasmic kinase domain of SIF2 (SIF2-CD), SLAC1 N-terminal coding region from amino acids 1 to 186 (SLAC1-N), and SLAC1 C-terminal domain from amino acids 501 to 556 (SLAC1-C) were expressed and purified in *E. coli*. As a negative control, the kinase-inactive form with the N683D mutation (SIF2-KD) was used. Kinase activity was determined by the incorporation of radiolabeled phosphate from [γ-^{32}P] ATP into the test peptide. A strong phosphorylation of SLAC1-N and a very mild phosphorylation of SLAC1-C by SIF2-CD were observed (Figure 6). The negative control SIF2-KD did not phosphorylate SLAC1 (Figure 6). These data suggest that SIF2 can phosphorylate the N-terminal domain of SLAC1.

SIF2 Is Required for the Activation of ABA-Induced S-Type Anion Channel Activity

Phosphorylation induces activation of SLAC1 anion channels, mediating anion efflux, membrane depolarization, and stomatal closure (Vahisalu et al., 2008; Geiger et al., 2009). We applied steady-state whole-cell patch clamp to investigate the effect of SIF2 disruption on ABA activation of S-type anion channels in guard cell protoplast. ABA treatment induces S-type anion currents in wild-type guard cell protoplast (Figure 7). By contrast, the current induced by ABA in the *sif2-1* mutant is indistinguishable from mock treatment (ethanol), indicating that SIF2 acts as an upstream activator of anion channels such as SLAC1.

Figure 2. (continued).

(B) D683N substitution abolished SIF2 autophosphorylation activity. SIF2 cytoplasmic kinase domain (SIF2-CD) and a kinase dead version with D683N substitution (SIF2-KD) were expressed in *E. coli.* Phosphorylation was revealed by SDS-PAGE and α-pThr immunoblotting. Coomassie Brilliant Blue (CBB) is used as loading control. This experiment was repeated twice with similar results.

(C) Overexpression of SIF2 dead kinase does not complement the hypersusceptibility phenotype of *sif2-1*. The Col-0 wild type (WT), *sif2-1*, CO1, and two lines overexpressing the SIF2 kinase dead in *sif2-1* (KD1 and KD2) were dip-inoculated with 10^6 cfu/mL *Pst* DC3000 for 15 min, and bacterial titers were evaluated at 2 DAI. Values represent average ± SEM from three independent experiments, each with three plants and three leaves from each plant (9 plants, $n \geq 9$). Asterisks indicate significant differences from the Col-0 wild type determined by a paired two-tailed *t* test ($P < 0.05$).

(D) to **(F)** The SIF2 dead kinase cannot complement *sif2-1*defective stomatal closure. Epidermal peels were floated in a suspension of 10^8 cfu/mL *Pst* DC3000 in 10 mM $MgSO_4$ **(D)** or treated with flg22 **(E)** or ABA **(F)** at the indicated concentrations. Stomatal openings were evaluated after 1 h in plant lines described in **(C)**. Values represent average ± SEM from three independent experiments, each consisting of at least 70 stomata from peels of three plants (9 plants, $n \geq 210$). Asterisks indicate significant differences from respective Col-0 wild type determined by a paired two-tailed *t* test ($P < 0.001$).

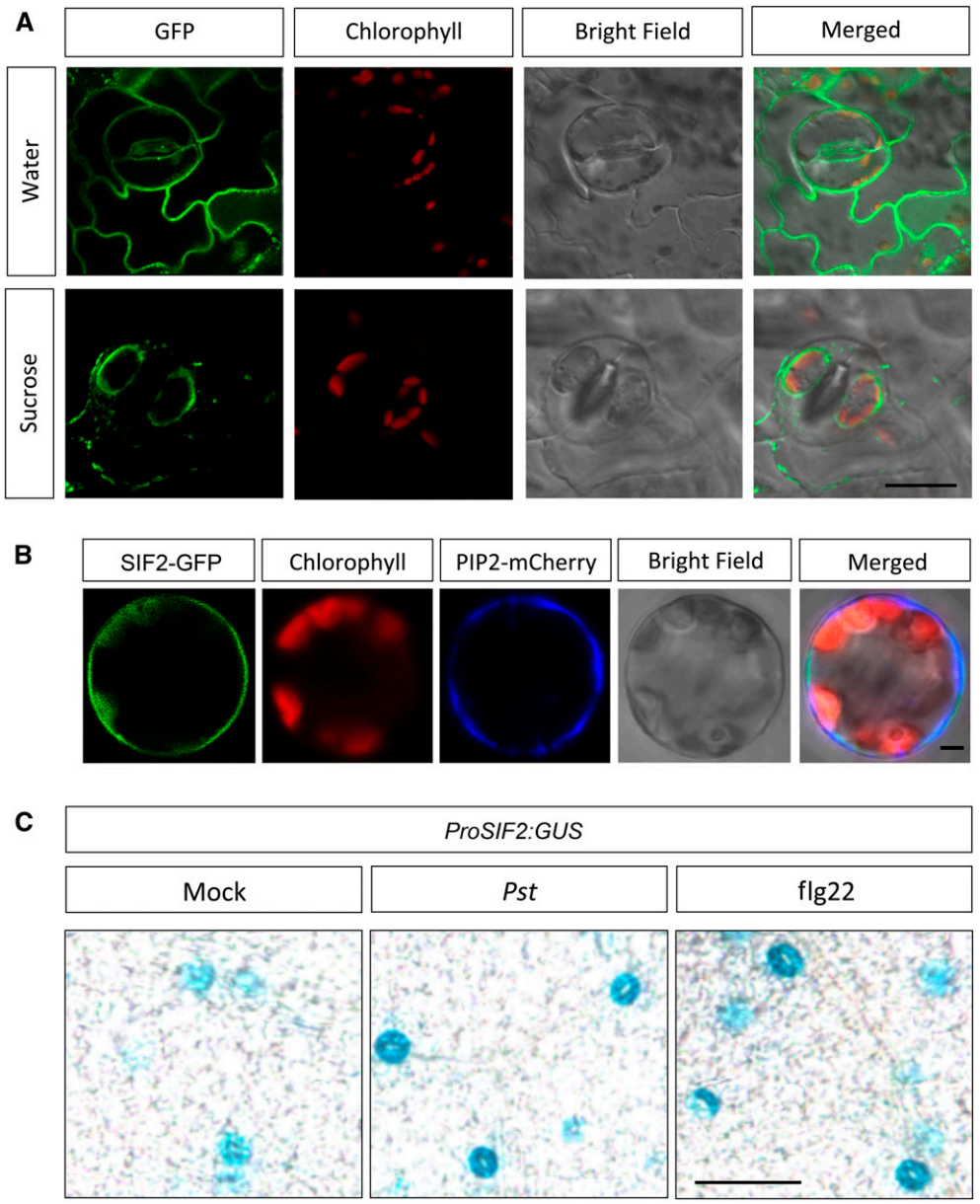

Figure 3. SIF2 Localization.

(A) SIF2 is localized at the plasma membrane. 10-d-old seedlings of the SIF2 overexpression line OE2 were used for imaging. Plasmolysis (Suc) is shown to visualize the plasma membrane localization. Similar observations were made in three random views and in another independent repeat. Scale bar = 20 μm.
(B) SIF2-GFP colocalized with PIP2-mCherry on the plasma membrane of mesophyll cell protoplast. OE2 protoplast was transfected with 35S:PIP2-mCherry. The GFP fluorescence (green), chlorophyll autofluorescence (red), mCherry fluorescence (blue), bright-field, and combined images were visualized under a confocal microscope after 16 h. Representative images of protoplasts from three random views and three independent experiments are shown. Scale bar = 10 μm.
(C) *SIF2* is expressed in guard cells. *ProSIF2:GUS* activity is visible in guard cells and GUS activity is increased after inoculation with 10^8 cfu/mL *Pst* DC3000 or treatment with 1 μM flg22. Pictures were taken 1 h after flg22 and at 1 hpi with *Pst* DC3000. The experiment was repeated twice with similar observations. Scale bar = 50 μm.

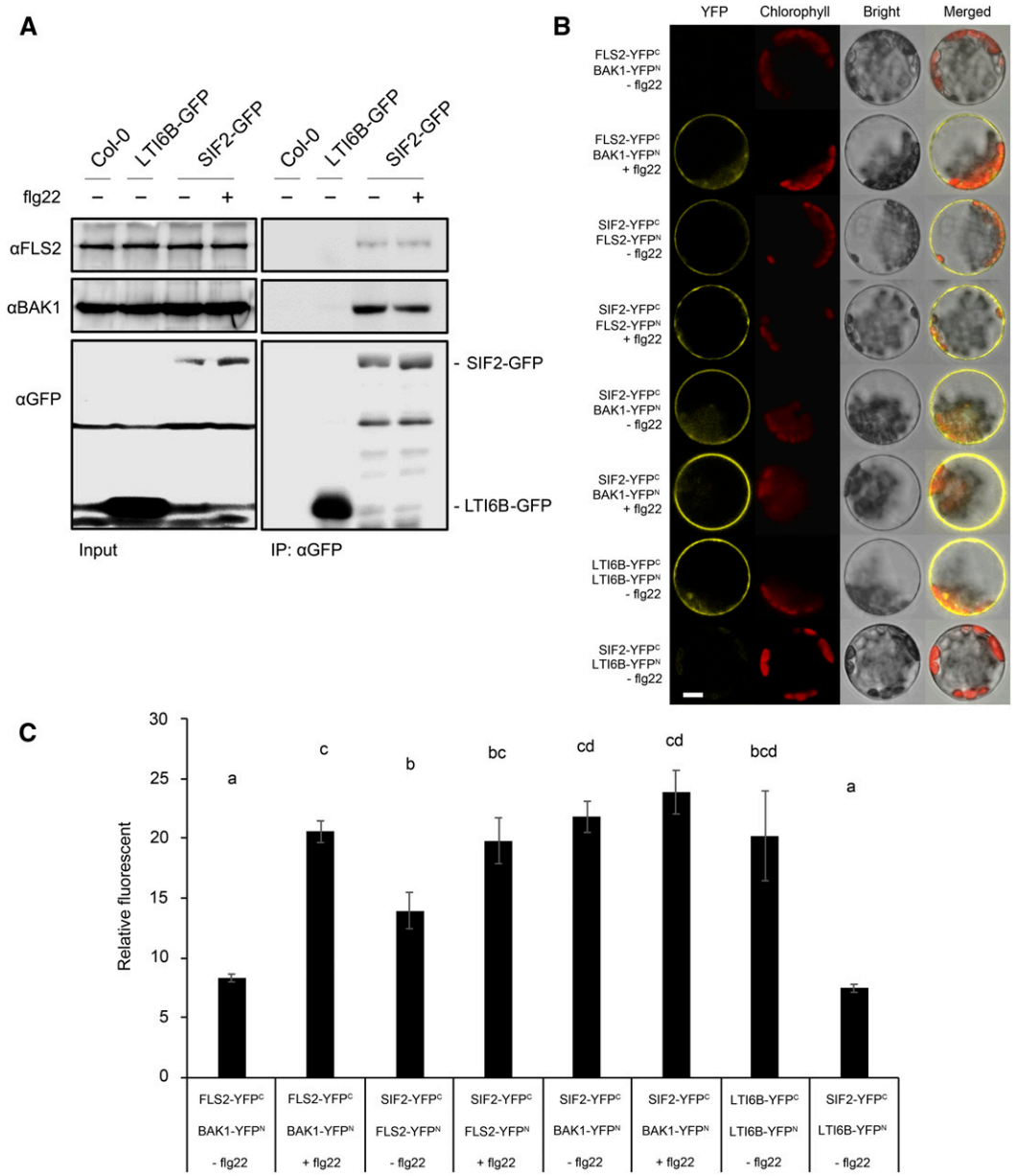

Figure 4. SIF2 Associates with Unstimulated and Stimulated FLS2 and BAK1.

(A) In planta ligand-independent association of SIF2 with FLS2 and BAK1. Transgenic Arabidopsis seedlings overexpressing SIF2-GFP (OE2) were treated (+) or not (−) with 100 nM flg22 for 10 min. For the CoIP, SIF2-GFP was immunoprecipitated with anti-GFP magnetic beads. Endogenous FLS2 and BAK1 were detected by α-BAK1 and α-FLS2 immunoblotting. As a negative control, plants overexpressing LTI6B-GFP were used. The experiment was repeated three times with similar observations.

(B) BiFC analysis of SIF2 interaction with FLS2 and BAK1. Arabidopsis protoplasts were cotransfected with FLS2-YFP^C + BAK1-YFP^N, SIF2-YFP^C + FLS2-YFP^N, SIF2-YFP^C + BAK1-YFP^N, LTI6B-YFP^C + LTI6B-YFP^N, or SIF2-YFP^C + LTI6B-YFP^N, and treated with (+) or without (−) 100 nM flg22 for 10 min. The YFP fluorescence (yellow), chlorophyll autofluorescence (red), bright-field, and combined images were visualized under an LSM 780 confocal microscope (Zeiss) after 16 h. Representative images of protoplasts from three random views and three independent experiments are shown. Scale bar = 10 μm.

(C) Fluorescence intensities of BiFC protoplasts. YFP fluorescence intensities of the brightest protoplasts are shown. Conditions were as described in **(B)**. Double-blind image analysis was performed with LSM software ZEN (Black edition). Values represent average ± SEM from three independent experiments (n = 50). Letters represent significant differences ($P < 0.05$) when analyzed by one-way ANOVA with post-hoc Tukey HSD.

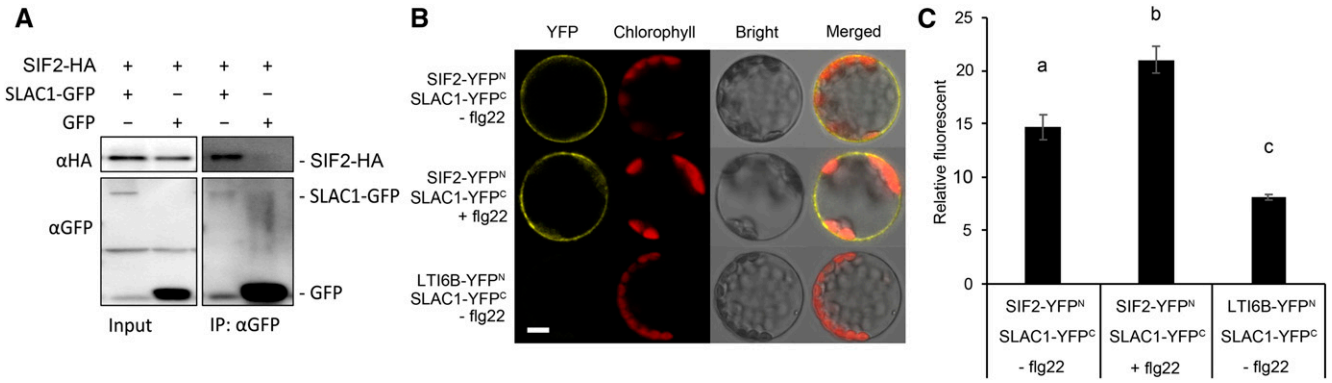

Figure 5. SIF2 Interacts with the Anion Channel SLAC1.

(A) CoIP analysis of SIF2 association with SLAC1 in Arabidopsis protoplasts. SIF2-HA_3 construct was cotransfected to protoplasts together with SLAC1-GFP (lane 1) or GFP only (lane 2). Total proteins were subjected to immunoprecipitation with anti-GFP magnetic beads. The presence of SIF2-HA_3 was detected by α-HA immunoblotting. The experiment was repeated three times with similar observations.

(B) BiFC analysis of SIF2 interaction with SLAC1. Arabidopsis protoplasts were cotransfected with SIF2-YFP^N + SLAC1-YFP^C or LTI6B-YFP^N + SLAC1-YFP^C, and treated with (+) or without (−) 100 nM flg22 for 10 min. The YFP fluorescence (yellow), chlorophyll autofluorescence (red), bright-field, and combined images were visualized under a confocal microscope after 16 h. Representative images of protoplasts from three random views and three independent experiments are shown. Scale bar = 10 μm.

(C) Fluorescence intensities of BiFC protoplasts. YFP fluorescence intensities of the brightest protoplasts are shown. Conditions were as described in **(B)**. Double-blind image analysis was performed with LSM software ZEN (Black edition). Values represent average ± SEM from three independent experiments ($n = 50$). Letters represent significant differences ($P < 0.05$) when analyzed by one-way ANOVA with post-hoc Tukey HSD.

SIF2-Mediated Stomatal Closure Depends on SLAC1 but Not OST1

Since SIF2 associates with the anion channel SLAC1 (Figure 5), transphosphorylates SLAC1 (Figure 6), and is required for anion channel activity (Figure 7), we tested whether SIF2-mediated stomatal closure depends on SLAC1 and the other well-known player in stomatal closure, OST1 (Geiger et al., 2009; Vahisalu et al., 2010; Brandt et al., 2012). Since overexpression of *SIF2* leads to constitutive stomatal closure (Supplemental Figure 4A), plants overexpressing SIF2 in *slac1-4* and *ost1-2* mutant backgrounds were analyzed for a possible constitutive stomatal closure phenotype. OE2 was used as a positive control. BASTA-resistant T1 individuals with decreasing *SIF2* expression levels (Supplemental Figure 13A and 13B) were used for this assay. As expected, stomata in OE2 were constitutively closed, while *slac1-4* and *ost1-2* stomata were open at a wild-type level (Figures 8A and 8B). Overexpression of *SIF2* in *slac1-4* did not induce stomatal closure in all the three transgenic lines tested (Figure 8A), indicating that SLAC1 is required for SIF2-mediated stomatal closure. On the other hand, lines overexpressing *SIF2* in *ost1-2* showed constitutive stomatal closure (Figure 8B). By contrast, OE/*ost1*-k, a transgenic line with low *SIF2* expression levels, harbored a wild-type stomata phenotype (Figure 8B). These data suggest that SIF2-mediated stomatal closure depends on SLAC1, but not on OST1.

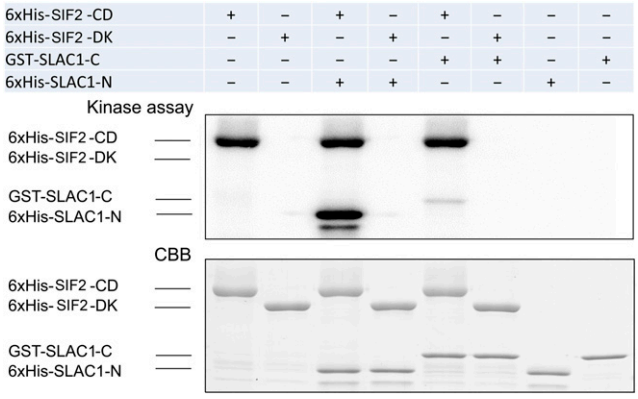

Figure 6. SIF2 Phosphorylates the SLAC1 N-Terminal Peptide In Vitro.

The cytoplasmic domain of SIF2 (SIF2-CD) was expressed and purified in *E. coli*. As a negative control, the dead kinase version with N683D mutation (SIF2-KD) is shown. The test peptide SLAC1-N (amino acid 1 to 186) and SLAC-C (amino acid 501 to 556) were produced similarly. Coomassie Brilliant Blue (CBB) staining was used as a loading control. The experiment was repeated twice with similar observations.

SIF2 Phosphorylates Specific SLAC1 Ser Residues

Based on in vivo interaction (Figure 5), in vivo function (Figure 7), and in vitro phosphorylation (Figure 6) analyses, the identification of specific phosphorylation sites of SLAC1 by SIF2 using in vitro phosphoproteomics coupled with electrophysiology was performed. Trypsin-digested SLAC1-N, phosphorylated by SIF2, was analyzed by high-pressure liquid chromatography coupled to tandem mass spectroscopy (LC-MS/MS) using nanospray ionization. Potential SIF2-mediated phosphorylation sites of SLAC1 were identified (Figure 9A).

Ser to Ala mutants were designed for all the potential phosphorylation sites, and these mutant constructs were tested for SIF2-mediated SLAC1 activation using oocyte patch clamp. SIF2

with the wild-type SLAC1 or SLAC1 mutants were coexpressed in oocytes, and macroscopic anion currents were measured (Figure 9B; Supplemental Figure 14). OST1 with SLAC1 wild type was used as a positive control, and SLAC1 wild type without kinase was used as a negative control (Figure 9B; Supplemental Figure 14). As expected (Geiger et al., 2009; Brandt et al., 2012), we observed significant current induction in OST1/SLAC1 wild type (Figure 9B; Supplemental Figure 14). Similarly, significant current induction in SIF2/SLAC1 wild type when compared to SLAC1 wild type alone was observed (Figure 9B; Supplemental Figure 14), suggesting that SIF2 can activate SLAC1. When SIF2 was coexpressed with SLAC1 mutants, significant current reduction was observed in SIF2/SLAC1 S65A when compared to SIF2/SLAC1 wild type (Figure 9B; Supplemental Figure 14), indicating that S65 is important for SIF2 to activate SLAC1. To date, the only characterized residues important for SLAC1 activity are Ser59 and Ser120, required by CPK6 (Brandt et al., 2012) and OST1 (Geiger et al., 2009; Vahisalu et al., 2010), respectively. This work thus identified an additional Ser residue crucial for SLAC1 activation.

To confirm the physiological significance of SLAC1 phosphorylation sites, we first generated 6xHis-SLAC1-N-6A (all six sites to A) and tested SIF2-mediated transphosphorylation in vitro. As expected, SIF2 transphosphorylated 6xHis-SLAC1-N, but phosphorylation of 6xHis-SLAC1-N-6A was strongly reduced (Figure 9C). Next, we asked whether the phosphomimicking SLAC1 gives a constitutive stomatal closure phenotype. Toward this goal, the *slac1-4* mutant was transformed with SLAC1-6D-GFP (all six sites to D) constructs and T1 individuals harboring GFP-positive transgene expression (Figure 9D), were evaluated for their stomatal immunity response to flg22 (Figure 9E). As expected, wild-type stomatal closure was observed in Col-0 plants, and *slac1-4* mutants were irresponsive to 100 nM flg22 (Figure 9E). In addition, the wild-type SLAC1 transgene successfully complemented the stomatal closure defect of *slac1-4* in response to flg22 treatment (Figure 9E). By contrast, stomata of SLAC1-6D/*slac1-4* transgenics were already closed before treatment with flg22 (Figure 9E), suggesting a constitutive stomatal closure in these transgenic lines. Consistent with this, patch-clamp experiments using oocytes with the SLAC1-6D construct showed constitutive activation of SLAC1 without the addition of an active kinase (Figure 9F). These data suggest that the SLAC1 Ser/Thr

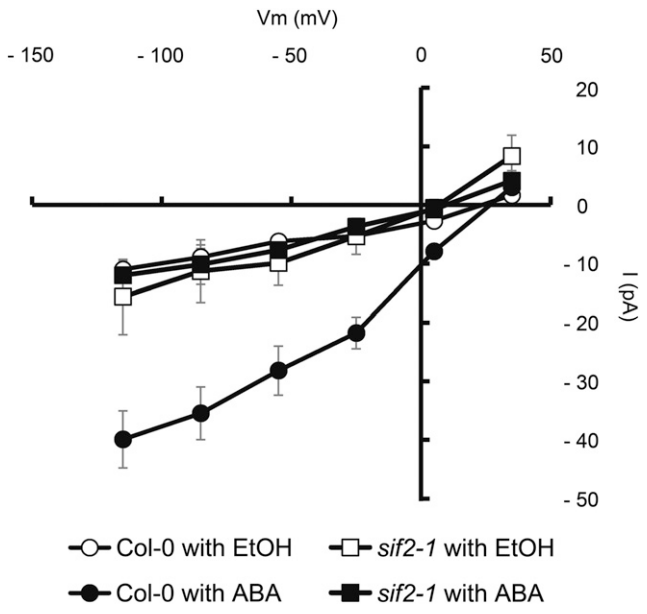

Figure 7. SIF2 Is Required for ABA-Mediated Activation of S-type Anion Channels.

Patch-clamp whole-cell recording of S-type anion channel currents in Arabidopsis guard cell protoplast of Col-0 wild type and *sif2-1* were performed with or without 50 μM ABA in the bath solution. Equivalent volumes of ethanol were used as mock controls. Values represent average ± SD ($n = 3$).

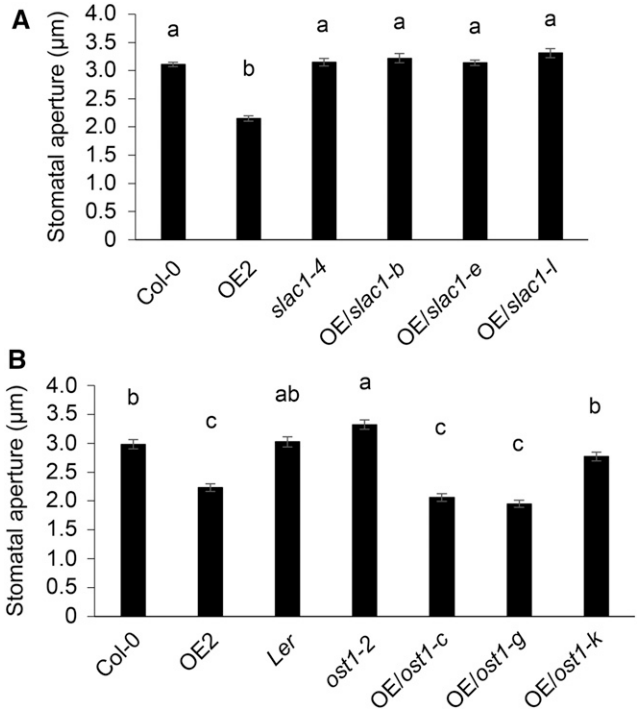

Figure 8. *SIF2*-Mediated Stomatal Closure Depends on SLAC1 but Not OST1.

(A) *SIF2*-mediated stomatal closure is abolished in the *slac1* mutant background. Epidermal peels of 5-week-old plants were floated in stomatal buffer, and stomatal openings were evaluated after 2.5 h. OE/*slac1*-b, OE/*slac1*-e, and OE/*slac1*-l are BASTA-resistant T1 plants overexpressing *SIF2* in the *slac1-4* mutant background. Values represent average ± SEM from three independent experiments, each consisting of at least 50 stomata from peels of three leaves (9 leaves, $n \geq 150$). Letters represent significant differences ($P < 0.05$) when analyzed by one-way ANOVA with post-hoc Tukey HSD.

(B) *SIF2*-mediated stomatal closure is retained in the *ost1* mutant background. OE/*ost1*-c, OE/*ost1*-g, and OE/*ost1*-k are BASTA resistant T1 plants overexpressing *SIF2* in *ost1-2* mutant background. Landsberg *erecta* (L*er*) is the wild-type background of *ost1-2*. Stomatal assays and statistical analyses were performed as in **(A)**.

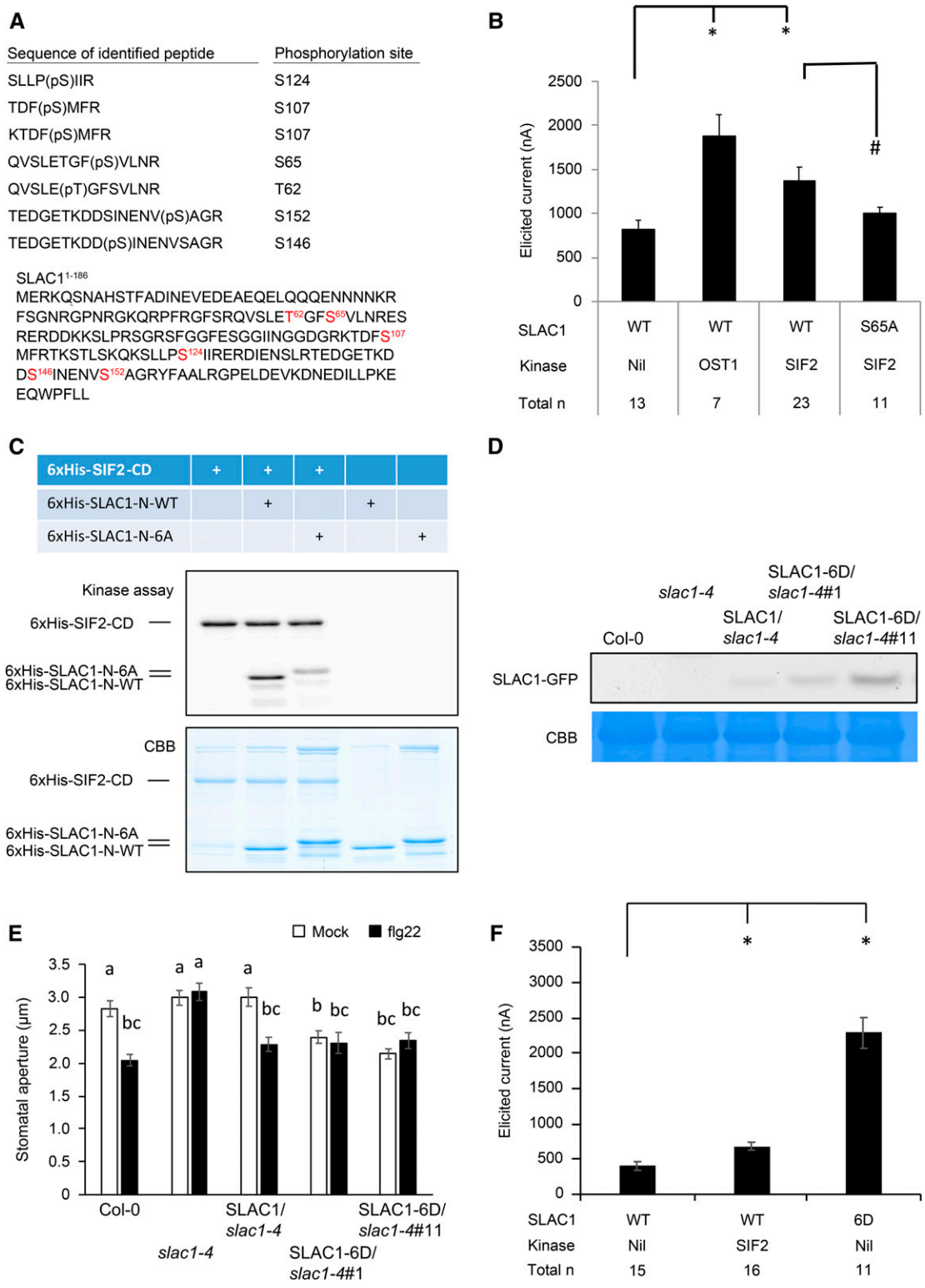

Figure 9. SIF2 Activates SLAC1 through Specific Phosphorylation Sites.

(A) Identification of putative SLAC1 phosphorylation sites by LC/MS-MS.

(B) A mutation in S65 decreases SIF2-mediated current intensity. Elicited currents were measured by two-electrode voltage-clamp (TEVC) using *Xenopus* oocytes injected with indicated SLAC1 variants and kinases. Values represent means ± SEM. The total n numbers are merged data from six independent

sites identified by LC-MS/MS are critical for SIF2-mediated phosphorylation, stomatal closure, and activation of SLAC1.

DISCUSSION

A reverse genetic approach with LRR-RLKs that are MAMPs or bacteria responsive (Postel et al., 2010) allowed us to identify the ML-RLK SIF2 as an important player in the Arabidopsis defense response against bacteria and notably in stomatal immunity (Figure 1). Importantly, this work suggests a model where SIF2 is required for ABA- and flg22-mediated stomatal closure through interaction with and phosphorylation of the guard cell anion channel SLAC1 (Figure 10). Supporting its role in stomata, histochemical GUS analyses revealed that the *SIF2* promoter was active in guard cells (Figure 3C). Since *sif2-1* showed defective stomatal immunity and stomata of *SIF2* OE lines were hyper-responsive to bacteria and flg22, we concluded that SIF2 acts as a positive regulator of stomatal immunity. Known regulators of the stomatal immunity response include members of the lectin receptor kinase family (Desclos-Theveniau et al., 2012; Singh et al., 2012; Arnaud and Hwang, 2015) and IOS1, another ML-RLK involved in PTI (Yeh et al., 2016); bacterial effectors and targets, such as HopM1 (Lozano-Durán et al., 2014) and RIN4 (Lee et al., 2015); regulators of endocytosis such as CHC2 (Mbengue et al., 2016) and ESCRT-I (Spallek et al., 2013); as well as SUSCEPTIBLE TO CORONATINE-DEFICIENT PST DC3000 (Zeng et al., 2011). This increasing number of stomatal immunity players, including SIF2, illustrates the critical role of stomata in the Arabidopsis defense response against bacteria. SIF2 was shown to act in ABA-, but not in SA-dependent signaling (Figure 1E; Supplemental Figure 8). Although an ABA-independent oxylipin pathway regulates stomatal immunity (Montillet et al., 2013), ABA nonetheless plays a central role in MAMP-induced stomatal closure (Melotto et al., 2006; Desclos-Theveniau et al., 2012; Lim et al., 2015; Lim and Lee, 2015). In contrast to the overexpression of the ML-RLK IOS1, which did not affect mock-treated stomatal closure (Yeh et al., 2016), overexpression of SIF2 induced constitutive stomatal closure. Plants overexpressing LecRK-VI.2 (Singh et al., 2012) or BAK1 (Domínguez-Ferreras et al., 2015) show constitutive activation of defense mechanisms. Similarly, the higher-than-normal SIF2 protein concentrations in OE lines may overcome negative regulatory players such as LecRK-V.5 (Desclos-Theveniau et al., 2012), inducing a constant stimulus leading to constitutive stomatal closure. Although we did not uncover a role for SIF2 in most apoplastic PTI responses (Supplemental Figures 6 and 7), a recent study showed that At1g51850 might be involved in early and late apoplastic PTI (Yuan et al., 2018). The *STRESS INDUCED FACTOR* (*SIF*) gene family encodes four leucine-rich repeat RLKs, *SIF1* to *SIF4*, which are differentially regulated under abiotic and biotic stresses (Yuan et al., 2018). In accordance with these recent results, flg22-mediated callose deposition was defective in the *sif2-1* mutant, and *SIF2* OE lines showed high callose levels (Supplemental Figures 7E and 7F). Thus, the basal level of *SIF2* expression in mesophyll cells (Winter et al., 2007; Yuan et al., 2018) and hence its contribution to Arabidopsis bacterial resistance through apoplastic mechanisms cannot be excluded.

Since SIF2 is involved in stomatal immunity and specifically in flg22-mediated stomatal closure, we further investigated the role of SIF2 in PTI by testing whether SIF2 is part of the FLS2-BAK1 PRR complex that recognizes the MAMP flg22 (Sun et al., 2013). Toward this goal, associations of SIF2 with FLS2 and the regulatory LRR-RLK BAK1 were evaluated by CoIP and BiFC analyses (Figure 4; Supplemental Figure 10). In planta CoIP experiments performed with Arabidopsis transgenic lines overexpressing SIF2-GFP showed that SIF2 constitutively associated with FLS2 and BAK1 and that elicitation with flg22 did not affect the association further (Figure 4A). BiFC analyses further suggested a ligand-independent direct interaction of SIF2 with FLS2 and BAK1 (Figures 4B and 4C), supporting the idea that SIF2 is part of the FLS2-BAK1 PRR complex. A growing number of Arabidopsis proteins are suggested to belong to PRR complexes independently of elicitation. For example, heterotrimeric G proteins (Liang et al., 2016), the cytoplasmic kinases BOTRYTIS-INDUCED KINASE 1 (BIK1)/PBS1-like and BRASSINOSTEROID-SIGNALING KINASE 1 (Lu et al., 2010; Zhang et al., 2010; Shi et al., 2013), PTI-COMPROMISED RECEPTOR-LIKE CYTOPLASMIC KINASE 1 (PCRK1) and PCRK2 (Kong et al., 2016), and the DENN domain protein STOMATAL CYTOKINESIS DEFECTIVE 1 (Korasick et al., 2010) directly interact with FLS2 to regulate PTI. The positive regulator of PTI, LecRK-VI.2 (Singh et al., 2012), also associates

Figure 9. (continued).

experiments. The asterisk indicates a significant difference ($P < 0.05$) when compared to the SLAC1 wild-type-injected oocytes. The number sign (#) indicates a significant difference ($P < 0.05$) to the oocytes coinjected with SLAC1 wild type and SIF2. Statistical analyses were performed by a paired two-tailed Student's *t* test.

(C) SIF2 cannot fully phosphorylate a SLAC1 N-terminal peptide mutated in the six putative phosphorylation sites described in **(A)**. The recombinant proteins 6xHis-SIF2-CD, 6xHis-SLAC1-N-WT, and 6xHis-SLAC1-N-6A were used to perform an in vitro phosphorylation assay as described in Figure 6. Coomassie Brilliant Blue (CBB) staining was used as a loading control. The experiment was repeated twice with similar results.

(D) SLAC1-GFP transgene expression. Total proteins of Col-0 wild type, *slac1-4*, SLAC1-GFP/*slac1-4*, SLAC1-6D/*slac1-4*#1, and SLAC1-6D/*slac1-4*#11 were subjected to SDS-PAGE and analyzed by anti-GFP immunoblotting. CBB staining was used as a loading control.

(E) Stomata of *slac1-4* transformed with SLAC1 constructs mutated to D in the six putative phosphorylation sites from **(A)** are constitutively closed. Epidermal peels were floated in stomatal buffer (mock) or treated with flg22, and stomatal openings were evaluated after 1 h. SLAC1/*slac1-4*, SLAC1-6D/*slac1-4*#1, and SLAC1-6D/*slac1-4*#11 are BASTA resistant T1 plants. Values represent average ± SEM from two independent experiments, each consisting of at least 30 stomata from peels of three leaves (6 leaves, $n \geq 60$). Letters represent significant differences ($P < 0.05$) when analyzed by one-way ANOVA with post-hoc Tukey HSD.

(F) Constitutive high currents by SLAC1-6D mutation. Elicited currents were measured by two-electrode voltage-clamp using *Xenopus* oocytes as in **(B)**. Values represent means ± SEM. The total *n* numbers are merged data from three independent experiments. The asterisk indicates a significant difference ($P < 0.05$) when compared with the SLAC1 wild type-injected oocytes. Statistical analyses were performed by a paired two-tailed Student's *t* test.

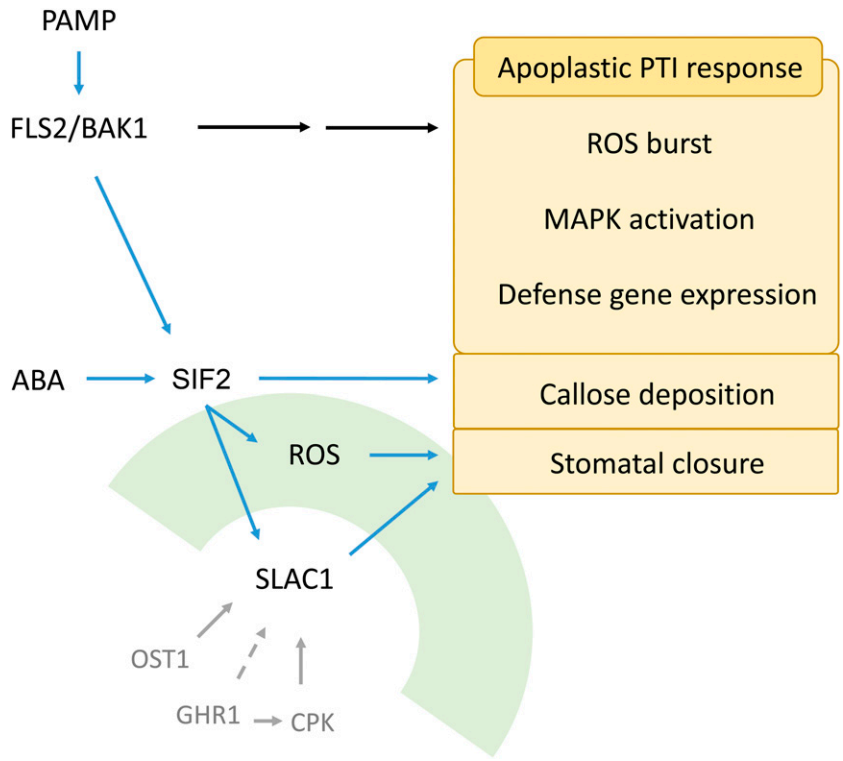

Figure 10. A Model for the Role of SIF2 in Innate Immunity.

SIF2 associates with the FLS2/BAK1 receptor complex on the plasma membrane. Stomatal closure upon bacteria, flg22, and ABA perception requires functional SIF2. SIF2 is also required for apoplastic callose deposition, but not for other aspects of apoplastic PTI responses such as ROS burst, MAPK activation, and defense gene expression. SIF2 expression is predominantly in the guard cell after MAMP perception, which is critical for ROS production in the guard cell, SLAC1 phosphorylation, and activation that leads to stomatal closure. SLAC1 is known to be regulated by multiple kinases through phosphorylation, including OST1, GHR1, and CPKs.

with FLS2 in a ligand-independent manner (Huang et al., 2014), and the SIF2 homolog IOS1 belongs to the FLS2 PRR complex, too (Yeh et al., 2016). This study thus uncovered a component of the FLS2 PRR complex.

Like the RLK GHR1 (Hua et al., 2012), SIF2 regulates guard cell movement. Importantly, GHR1 interacts with SLAC1 (Hua et al., 2012), a key S-type anion channel in ABA-dependent stomatal signaling (Negi et al., 2008; Vahisalu et al., 2008), to regulate dehydration stress and stomatal closure triggered by the air pollutant ozone and elevated CO_2 (Sierla et al., 2018). We thus asked whether SIF2 also interacts with SLAC1. CoIP and BiFC analyses in Arabidopsis protoplasts suggested that SIF2 associates (CoIP) and directly interacts (BiFC) with the anion channel SLAC1 (Figure 5).

As predicted, SIF2 possesses an active kinase domain required for its in planta function. This observation suggests that SIF2 function in stomatal regulation is primarily exerted through its kinase activity. Supporting this hypothesis, phosphorylation cascades are known to be key in signaling events (Murata et al., 2015). For example, the kinase activity of the multipurpose coreceptor BAK1 is required for both defense and growth regulation (Wang et al., 2008; Schwessinger et al., 2011). However, since ML-RLKs can function through other mechanisms than substrate phosphorylation, such as extracellular domain cleavage for SYMBIOSIS RECEPTOR-LIKE KINASE (SYMRK; Antolín-Llovera et al., 2014), we cannot exclude other mechanisms of action for SIF2.

Activation of the SLAC1 ion channel requires phosphorylation by an active kinase (Chen et al., 2010). Specific phosphorylation sites have indeed been identified, including Ser120 phosphorylation by OST1 (Vahisalu et al., 2010) and Ser59 phosphorylation by CPK6 (Brandt et al., 2012). Observed N-terminal phosphorylation of SLAC1 by SIF2 (Figure 6) provides important evidence to fill the missing link between MAMP elicitation of guard cells and stomatal closure upon activation of stomatal immunity. Of note, activation of SLAC1 through N-terminal phosphorylation is common (Geiger et al., 2009; Brandt et al., 2012). SIF2 thus appears to regulate SLAC1 similarly to OST1 and CPK6. Using the patch-clamp technique in *sif2-1* guard cell protoplasts and in oocytes, we confirmed the essential role of SIF2 in mediating ABA-dependent S-type anion channel activation (Figures 7 and 9). Notably, we identified the putative phosphorylation site Ser65 as critical for SIF2-mediated SLAC1 activation. The repression in Ser65 mutant is strong, suggesting that the Ser65 site is critical for SLAC1 activity, at least under the action of SIF2.

A genetic approach confirmed that SIF2 mediates stomatal closure through SLAC1. Loss of SLAC1 function in *slac1-4* mutant indeed abolished the constitutive stomatal closure phenotype

observed in SIF2 overexpression lines (Figure 8A). SLAC1 appears to be regulated by multiple kinases through phosphorylation, including GHR1 (Hua et al., 2012), OST1 (Geiger et al., 2009; Vahisalu et al., 2010), CPK6 (Brandt et al., 2012), and SIF2. The specificity and relative importance for each kinase in response to various environmental cues remain largely unknown. Surprisingly, SIF2-mediated stomatal closure acted independently of OST1 (Figure 8B), a key player in ABA-mediated stomatal closure (Mustilli et al., 2002). Although SIF2 was shown to directly phosphorylate SLAC1, ABA-induced ROS production is lost in *sif2-1* guard cells (Figure 1F), suggesting that SIF2 acts upstream of ROS in controlling ABA-mediated stomatal closure. This regulation is guard cell specific, as the ROS burst during the apoplastic PTI response is at a wild-type level in the *sif2-1* mutant.

How can SIF2 regulate ROS production and directly phosphorylate SLAC1? SIF2 may function at multiple levels in the signaling pathway leading to ABA-mediated stomatal closure. In a similar manner, OST1 acts upstream of ABA-mediated ROS production (Mustilli et al., 2002) and directly phosphorylates SLAC1 (Vahisalu et al., 2010). In the ROS production signaling, OST1 regulates the activity of the NADPH oxidase AtrbohF through phosphorylation of AtrbohF Ser13 and Ser174 (Sirichandra et al., 2009). Since BIK1, another RLK associated with FLS2 (Lu et al., 2010; Zhang et al., 2010), directly phosphorylates the NADPH oxidase RbohD to control plant stomatal immunity (Kadota et al., 2014; Li et al., 2014), SIF2 may regulate RbohD activity in addition to the direct phosphorylation of SLAC1. SIF2-mediated phosphorylation of SLAC1 was strongly abolished when all Ser/Thr sites identified by LC-MS/MS were mutated to A (Figure 9C). In addition, a phosphomimicking version of SLAC1 with all LC-MS/MS identified sites mutated to Asp (6D) showing constitutive closure of stomata and high patch-clamp current (Figures 9E and 9F). Together, these data further underline the critical role of SIF2 on SLAC1 phosphorylation and in SLAC1-mediated stomatal closure. Overall, we present a comprehensive study of a receptor-like protein kinase, SIF2, which is required for ABA-mediated stomatal closure and stomatal immunity through interaction with and phosphorylation of the guard cell anion channel SLAC1.

METHODS

Growth Conditions and Biological Materials

Arabidopsis (*Arabidopsis thaliana*) plants were grown in commercial potting soil with perlite in 3:2 ratio, at 22 to 24°C day and 17 to 19°C night temperature, under ~100 μE m^{-2} s^{-1} illumination using bulb-type fluorescent light with 9-h light/15-h night photoperiod. The T-DNA insertion mutant *sif2-1* (SALK_068030) and *slac1-4* (SALK_137265) are in the ecotype Columbia (Col-0) background. *sif2-1* and *slac1-4* seeds were obtained from the Arabidopsis Biological Resource Center (ABRC; http://abrc.osu.edu/; Alonso et al., 2003). Genotyping was performed by PCR amplification of insertion-specific or wild-type-specific DNA fragments with primers listed in Supplemental Table 1. *ost1-2* seeds were used in a previous publication (Yekondi et al., 2018). Plants were grown under standard conditions as previously described by Yeh et al. (2016).

Bacterial strain *Pseudomonas syringae* pv *tomato* DC3000 was kindly provided by Barbara N. Kunkel (Washington University, St. Louis, Missouri). The fungus *Botrytis cinerea* (B071) was obtained from Chao-Ying Chen (National Taiwan University, Taipei, Taiwan). Bacteria were cultured at 28°C and 200 rpm in King's B medium with 50 mg/L rifampicin. *B. cinerea* was grown at room temperature on potato dextrose agar plates as described by Zimmerli et al. (2001).

SIF2 Cloning, Overexpression, and Mutant Complementation

The full-length genomic sequence of *SIF2* was PCR amplified using primers spanning the predicted ATG to the stop codon (not included; SIF2-F and SIF2-R, Supplemental Table 2). The PCR product was cloned into pCR8/GW/TOPO vector (Invitrogen) and subsequently recombined into the Gateway-compatible destination binary vector pEarlyGate 103 (ABRC; http://abrc.osu.edu/), harboring the 35S promoter and a C-terminal GFP-6x-His tag, through the LR reaction according to the manufacturer's instructions (Invitrogen). The construct was transformed into Col-0 and *sif2-1* by *Agrobacterium tumefaciens* GV3101-mediated transformation (Clough and Bent, 1998) to generate OE and CO lines, respectively. Lines stably expressing *SIF2* transcript and protein, with single-insertion (T2, 3:1 segregation ratio) and homozygous (T3, no segregation) were used in subsequent experiments. The kinase-inactivating mutation D683N was introduced through primer extension (primers are listed in Supplemental Table 2) on the binary vector pEarleyGate103 containing the full-length *SIF2* genomic sequence. SIF2 dead kinase complemented lines were generated by transforming this construct into *sif2-1* using *A. tumefaciens* GV3101 as above.

Pathogen Infection Assays

Five-week-old plants were dip-inoculated for 15 min in 10^6 cfu/mL bacterial suspensions and then kept at 100% relative humidity for one night. Symptoms were evaluated 3 DAI. Bacterial titers were quantified on King's B agar plates as described previously (Yeh et al., 2016).

B. cinerea spores were diluted to 10^5 spores/mL in half-strength potato dextrose broth medium. Ten-microliter droplets of this suspension were deposited on leaf surfaces of three leaves per plant of 5-week-old plants. Leaves of the same age were used for droplet inoculation. Plants were then kept at 100% humidity, and disease symptoms and lesion perimeters were determined at 3 DAI (Zimmerli et al., 2001).

MAMP and Hormone Treatments

The flg22 peptide was purchased from Biomer Technology and dissolved in water. The concentrations used are indicated in each figure legend. Water-only treatment was used as mock control. ABA and SA were dissolved in 99% (v/v) ethanol to give 100 mM stock solution and diluted in water to the respective working concentrations. Equivalent volume of 99% (v/v) ethanol was used as mock control.

Stomatal Aperture Assay

Abaxial epidermal peels were collected from fully expanded leaves of 5-week-old plants and floated on stomatal buffer (25 mM MES/KOH, pH 6.15, 10 mM KCl). The peels were incubated for 3 h under light. The MAMPs flg22, chitin, and LPSs, H_2O_2, and the hormones ABA or SA were then added at the indicated concentrations. For mock treatments, equivalent volumes of water (MAMPs and H_2O_2) or 99% ethanol (ABA and SA) were added. For *Pst* DC3000 inoculation, stomatal buffer was exchanged with 10 mM $MgSO_4$ (mock) or with 10^8 cfu/mL bacterial suspension in 10 mM $MgSO_4$. The peels were mounted on microscope slides and imaged at the indicated time points with an Olympus BX51 microscope. The width of the stomatal aperture was measured using ImageJ (Wayne S. Rasband, ImageJ, NIH, https://imagej.nih.gov/ij/, 1997 to 2016). For each sample, peels from at least three plants were used as previously described by Tsai et al. (2011).

RT-qPCR

For MAMP-induced gene expression, 10-d-old seedlings were transferred to liquid half-strength Murashige and Skoog (MS) one night before flg22 treatments. Total RNA isolation, cDNA biosynthesis, and real-time PCR analyses were performed as described by Yeh et al. (2016). Normalization of gene expression was conducted with At4g05320 (*UBQ10*). Primers are listed in Supplemental Table 3.

MAP Kinase Assay

Seedlings were grown for 13 d on half-strength Murashige and Skoog plates and transferred to liquid half-strength Murashige and Skoog medium 1 d prior to flg22 treatment. Liquid half-strength Murashige and Skoog was changed to 0.5 μM flg22 in water or with sterile water only (mock) for 10 min. Samples were then snap frozen in liquid nitrogen. MAP kinase assay was performed as described by Singh et al. (2012).

ROS Burst

The ROS assay was performed as described by Huang et al. (2013). In brief, nine 0.25 cm^2 leaf discs were excised from fully expanded leaves of three 5-week-old plants. The discs were incubated overnight in a 96-well plate with 100 μL of sterile water. The water was then replaced with 100 μL reaction solution (2 μM luminol [Sigma-Aldrich], 10 μg/mL horseradish peroxidase [Sigma-Aldrich]) and 100 nM flg22 or water (mock). The plate was analyzed at the indicated intervals for a period of 30 min using a CentroLIApc LB 692 plate luminometer (Berthold Technologies).

Callose Deposition

Twelve leaf discs of 5-week-old plants were collected 9 h postin-infiltration with 1 μM flg22 diluted in sterilized water. Sterilized water was used as mock control. Harvested leaf samples were cleared overnight by incubation in 95% (v/v) ethanol at room temperature and then washed three times (2 h for each washing) with sterilized water. Cleared leaf discs were stained with 0.01% (w/v) aniline blue in 0.15 M phosphate buffer, pH 9.5, for 24 h. Callose deposits were visualized under UV light illumination using an Olympus BX51 microscope. Quantification of callose deposits was performed on the acquired digital images using ImageJ (W.S. Rasband, ImageJ, NIH, https://imagej.nih.gov/ij/, 1997 to 2016).

Measurement of ROS Production in Guard Cells

ROS in guard cells were analyzed as previously described by Desclos-Theveniau et al. (2012) with modifications. In brief, epidermal peels were incubated in stomatal buffer (25 mM MES/KOH, pH 6.15, 10 mM KCl) for 2.5 h before transfer to 50 μM H2DCFDA in 10 mM Tris-HCL, pH 7.2, for 15 min. The peels were then washed three times in 10 mM Tris-HCl, pH 7.2. One μM ABA or 1 μM SA were then added, and H2DCFDA fluorescence was imaged at the indicated time points with an Olympus BX51 microscope with excitation at 460 to 480 nm and emission at 495 to 540 nm. Pixel intensity was evaluated by ImageJ (W.S. Rasband, ImageJ, NIH, https://imagej.nih.gov/ij/, 1997 to 2016) and normalized to initial fluorescence intensities.

Recombinant Protein and Autophosphorylation Assays

The *SIF2* kinase domain was amplified from the ABRC clone X1G51850AEHK and subcloned into pET-28a expression vector (Novagen). To produce an inactive version of the kinase, a D683N mutation at the kinase activation residue was introduced. The fusion proteins were expressed in *Escherichia coli* BL21 and purified with HisTrap FF column (GE Healthcare) according to manufacturer's instructions. Proteins were separated on 10% (w/v) SDS-PAGE and transferred on a polyvinylidene difluoride membrane (Immobilon-P; Millipore). Membranes were blocked with 3% (w/v) BSA in Tris-Buffered Saline and 0.1 % (v/v) Tween 20, followed by addition of primary antibody anti-pThr (1:10,000) and incubated overnight at 4°C. After washing three times with TBST, membranes were incubated with secondary antibody anti-rabbit horseradish peroxidase (1:5000) for 1 h at room temperature. After washing with TBST, signals were visualized with an enhanced chemiluminescence system (Immobilon Western, Millipore) and a LAS-3000 (Fujifilm) scanner following the manufacturer's instructions.

GUS Staining and Subcellular Localization

The ~1 kb promoter region of SIF2 was PCR amplified (primers are listed in Supplemental Table 4), subcloned into pCR8/GW/TOPO vector (Invitrogen), and subsequently recombined into pMDC163 vector (Curtis and Grossniklaus, 2003) by the LR reaction following the manufacturer's instruction (Invitrogen). The construct was transformed into Col-0 by *A. tumefaciens* GV3101-mediated transformation (Clough and Bent, 1998), and positive transformants were selected on half-strength Murashige and Skoog agar plates supplemented with 15 μg/mL hygromycin B. Seedlings were harvested in cold 90% (v/v) acetone, followed by vacuum infiltration for 10 min. The tissue was allowed to stand and fix at room temperature for 20 min. Acetone was then replaced by staining buffer without X-Gluc (50 mM phosphate buffer, 0.2% [v/v] Triton-X, 1 mM potassium ferrocyanide, 1 mM potassium ferricyanide) and vacuum infiltrated for 10 min. The buffer without X-Gluc was then replaced by staining buffer containing X-Gluc (50 mM phosphate buffer, 0.2% [v/v] Triton-X, 1 mM potassium ferrocyanide, 1 mM potassium ferricyanide, 2 mM X-Gluc) and incubated at 37°C overnight. Tissue was then washed successively in 25, 50, and 75% (v/v) ethanol series and imaged with an Olympus BX51 microscope.

GFP localization was observed by examining seedlings of the *SIF2* OE line OE2. In brief, 10-d-old seedlings of OE2 were mounted on microscopy slides with water, and GFP signal was captured with an LSM 780 confocal microscope (Zeiss). Plasmolysis was performed by preincubation of the seedlings with 25% Suc for 3 min. Colocalization by transient expression was performed by transforming OE2 protoplast with 35S:PIP2-mCherry construct using standard polyethylene glycol approach as described by Yeh et al. (2016).

BiFC Assay

SIF2 genomic sequence, full-length coding sequences of *FLS2*, *BAK1*, and *LTI6B* without stop codon, amplified from cDNA of Col-0 plants, were inserted into the entry vector pCR8/GW/TOPO and subcloned into YN (pEarleyGate201-YN) or YC (pEarleyGate202-YC) vectors (Lu et al., 2010) through the LR reaction (Invitrogen). The constructs were transfected into Arabidopsis protoplasts by polyethylene glycol (Sigma-Aldrich) for transient expression (Yoo et al., 2007). Sixteen hours later, transfected cells were treated with or without 100 nM flg22 for 10 min before being imaged using a Zeiss LSM 780 confocal microscope (Germany). Image analysis was performed with LSM software ZEN (Black edition). The experimenter and the person doing the analysis were different individuals.

CoIP and Immunoblotting

For protein extraction and immunoprecipitation, young leaves from 5-week-old Arabidopsis were used. The protocol for protein extraction is already described by Roux et al. (2011). For immunoprecipitation of SIF2-GFP, supernatants were incubated with 50 to 200 μL of anti-GFP magnetic beads (Miltenyi Biotec) for 2 h at 4°C (Kadota et al., 2014, 2016). Following incubation, beads were washed three to five times with TBS containing 0.5% (v/v) IGEPALCA-630 before adding SDS loading buffer

(Schwessinger et al., 2011). Endogenous BAK1 and FLS2 were detected by native antibody (Schulze et al., 2010).

Protein extraction and immunoprecipitation in Arabidopsis protoplasts were performed as described by Yeh et al. (2016). In brief, plasmids containing HA_3 or GFP tag constructs were cotransfected into Arabidopsis protoplasts by polyethylene glycol (Sigma-Aldrich) for transient expression (Yoo et al., 2007). Total proteins were extracted with 0.5 mL protein extraction buffer (50 mM Tris-HCl, pH 7.5, 150 mM NaCl, 10% [v/v] glycerol, 10 mM DTT, 10 mM EDTA, 1 mM NaF, 1 mM $Na_2MoO4 \cdot 2H_2O$, 1% [v/v] IGEPAL CA-630 [Sigma-Aldrich], and 1% [v/v] Roche protease inhibitor cocktail) and incubated with gentle shaking at 4°C for 1 h. Samples were then centrifuged at 14,000 rpm for 15 min (or as specified in figure legends, at 40,000 × *g* for 60 min using Optima L-1000K Ultracentrifuge, Beckman Coulter) at 4°C. Supernatants (1.5 mL) were adjusted to 2 mg/mL protein and incubated for 2 h at 4°C with 20 mL GFP Trap-A beads (Chromotek). Following incubation, beads were washed four times with TBS containing 0.5% (v/v) IGEPALCA-630. Total proteins (input) or immunoprecipitated proteins were separated by 10% (w/v) SDS-PAGE and then transferred to polyvinylidene difluoride membrane. GFP and HA_3 fusion proteins were detected by immunoblotting with anti-GFP and anti-HA primary antibodies, respectively.

In Vitro Kinase Assay

For in vitro kinase assays, SLAC1 C terminus was cloned into pGEX-4T-1 vector (GE Healthcare) with primers listed in Supplemental Table 5. The plasmid for the SLAC1 N-terminal coding region for amino acids 1 to 186 was established previously (Vahisalu et al., 2010). Proteins 6xHis-SLAC1-N, 6xHis-SIF2-CD (cytoplasmic domain), 6xHis-SIF2-KD (kinase dead), and GST-SLAC1-C were expressed in *E. coli* BL21 (DE3) cells. The cultures were grown in 2 × yeast extract tryptone medium at 37°C to OD600 ~0.6. Recombinant protein expression was induced with 0.4 mM isopropyl β- d-1-thiogalactopyranoside at 16°C for 16 h, and 6xHis-tagged proteins were purified by nickel-affinity chromatography. GST-tagged proteins were purified by glutathione-affinity chromatography. SIF2 kinase activity assay was performed by incubating 2 μg of purified recombinant SIF2 and SLAC1-N (5 μM) or GST-SLAC1-C (5 μM) in 10 μL reaction buffer (50 mM Tris-HCl [pH 7.4], 150 mM NaCl, 10 mM $MgCl_2$, 10 mM $MnCl_2$, 500 μM ATP, 1 mM DTT, 0.2 mg/mL insulin, and 100 μCi/mL 32P-γ-ATP) at room temperature for 30 min. Reactions were stopped by the addition of 3× SDS loading buffer. Proteins were separated by 10% (w/v) SDS-PAGE and visualized by Coomassie Brilliant Blue G-250 (Sigma-Aldrich) staining. SIF2 activity was determined by autoradiography.

Patch-Clamp Experiments with Arabidopsis Guard Cell Protoplasts

Arabidopsis guard cell protoplasts were isolated enzymatically from epidermal strips of 5-week-old plants. Standard whole-cell recordings were made using an Axoclamp 900A amplifier (Axon Instrument). Giga ohm seals (>10 GΩ) were obtained by suction. All assays were conducted at room temperature. The bath solution contained 30 mM CsCl, 2 mM $MgCl_2$, 10 mM MES-Tris (pH 5.6), and 1 mM $CaCl_2$, with an osmolarity of 485 mmol/kg. The pipette solution contained 5.58 mM $CaCl_2$, 6.7 mM EGTA, 2 mM $MgCl_2$, 10 mM HEPES-Tris (pH 7.1), and 150 mM CsCl, with an osmolarity of 500 mmol/kg. The final osmolarity in both bath and pipette solution was adjusted with D-sorbitol. Fresh Mg-ATP (5 mM) was added to the pipette solution before use. For analysis of the ABA activation of S-type anion channels, the guard cell protoplasts were preincubated with 50 μM ABA for 20 min before patch clamping, and patch-clamp experiments were performed in the presence of 50 μM ABA in the bath solution. S-type anion current was measured 10 min after whole-cell configurations became accessible. The membrane voltage was stepped to potential starting from +35 to −115 mV with 30-mV decrements, and the holding potential was 30 mV. The interpulse period was 10 s. Steady-state currents were the currents before 400 ms from the end of pulses.

LC-MS/MS

Purified recombinant 6xHis-NSLAC1 was phosphorylated by 6xHis-SIF2-CD. An aliquot from kinase reaction was pooled together with SDS-PAGE loading buffer (1:1). Proteins were separated by 10% (w/v) SDS-PAGE, the gel was stained with Coomassie Brilliant Blue G-250 (Sigma-Aldrich), and the NSLAC1 protein band was excised from gel. In-gel digestion of NSLAC1 protein was performed by Trypsin/P (10 ng μL^{-1}; Sigma-Aldrich). Peptides were purified with C18 StageTips and were loaded onto a fused silica emitter (75 μm × 150 mm, Proxeon) packed in house with Reprosil-Pur C18-AQ 3-μm particles (Dr. Maisch HPLC). Peptides were separated by Agilent 1200 series nanoflow system (Agilent Technologies) with a 30-min 3 to 40% buffer B (0.5% [v/v] acetic acid and 80% [v/v] acetonitrile) gradient at a flow rate of 200 nL min^{-1}, and eluted peptides were sprayed directly into an LTQ Orbitrap XL classic mass-spectrometer (Thermo Electron) with a spray voltage of 2.2 kV. The MS scan range was *m/z* 300 to 1,800, and the top five precursor ions were selected for subsequent MS/MS scans. A lock mass of 445.0003 was used for the LTQ Orbitrap to obtain constant mass accuracy during the gradient analysis.

Peptides were identified with the Mascot (http://www.matrixscience.com/) search engine. Peptide mass tolerance of 7 mg/kg and fragment ion mass tolerance of 0.5 D were used. Two missed cleavage sites for Trypsin/P was allowed. The carbamidomethylation of cysteine was set as fixed modification. The oxidation of Met and phosphorylation of Ser and Thr were set as variable modifications.

Site-Directed Mutagenesis and In Vitro Transcription

SLAC1, *SIF2*, *OST1*, *ABI1*, and *ABI2* coding sequences were subcloned into pGEMHE expression vector by standard approaches. Site-directed mutagenesis was performed using primers listed in Supplemental Table 6. The constructs were linearized with the appropriate restriction enzyme and purified by commercial kits. In vitro transcription was performed using mMESSAGE mMACHINE T7 transcription kit (Thermo Fisher Scientific). Twenty-five nanograms of cRNA, for each gene, in 50 nL diethyl pyrocarbonate-treated water was injected per cell.

Electrophysiological Analyses Using *Xenopus* Oocytes

The two-electrode voltage-clamp method was used to measure the elicited current from injected *Xenopus* oocytes. cRNA was transcribed in vitro using mMESSAGE mMACHINE kits (Amion). Oocytes were isolated, injected with 25 ng of SLAC1 cRNA with or without 25 ng of SIF2 cRNA in 50 nL of water, and incubated at 16°C for one day. The perfusion buffer and recording program are modified from previous study (Geiger et al., 2009; PNAS 106, 21,425). The perfusion buffer contained 10 mM MES/Tris (pH 5.6), 1 mM $CaCl_2$, 1 mM $MgCl_2$, 96 mM NaCl, and 12 mM Mannitol (220 mM osmolality). The microelectrodes were filled with 3 M KCl. Steady-state currents were recorded starting from a holding potential of 0 mV and ranging from +60 to −160 mV in 10-mV decrements for 100 ms, followed by a −120 mV pulse. The whole-cell currents were recorded by a Cornerstone (Dagan) TEV-200 two-electrode voltage-clamp amplifier. Data were processed with an Axon Instruments Digidata 1440A low-noise data acquisition system (Molecular Devices and Clampfit software).

Accession Numbers

Sequence data from this article can be found in the Arabidopsis Genome Initiative or GeneBank/EMBL data libraries under the following accession

numbers: At1g51850 (SIF2), At2g19190 (FRK1), At5g57220 (CYP81F2), At4g05320 (UBQ10), At1g12480 (SLAC1).

Supplemental Data

Supplemental Figure 1. SIF2 is necessary for full Arabidopsis resistance to hemibiotrophic bacteria

Supplemental Figure 2. Wild-type resistance of *sif2-1* mutant to *B. cinerea* infection

Supplemental Figure 3. SIF2 is not critical upon *Pst* DC3000 infiltration-inoculation

Supplemental Figure 4. The stomatal responses of SIF2 OE lines

Supplemental Figure 5. SIF2 is not required for LPS and chitin guard cell responses

Supplemental Figure 6. SIF2 does not play a role in early apoplastic PTI responses

Supplemental Figure 7. Late PTI responses

Supplemental Figure 8. SA-induced stomatal closure is not affected in the *sif2-1* mutant

Supplemental Figure 9. H_2O_2-induced stomatal closure

Supplemental Figure 10. CoIP analysis of SIF2 association with FLS2 and BAK1 in Arabidopsis protoplasts

Supplemental Figure 11. CoIP analysis of SIF2 and IOS1 association with SLAC1 in Arabidopsis protoplasts

Supplemental Figure 12. BiFC analysis of IOS1 interaction with SLAC1

Supplemental Figure 13. *SIF2* expression levels in *slac1-4* and *ost1-2* mutant backgrounds

Supplemental Figure 14. Functional analysis of SLAC1 mutants by *Xenopus* oocyte patch clamp

Supplemental Table 1. Primers for *sif2-1* genotyping

Supplemental Table 2. Primers to generate SIF2 full-length genomic sequence and dead kinase

Supplemental Table 3. Primers for real-time PCR

Supplemental Table 4. Primers for PCR amplification of the *SIF2* promoter

Supplemental Table 5. Primers for SLAC1 C-terminal subcloning

Supplemental Table 6. Primers for pGEMHE-SLAC1 mutagenesis

ACKNOWLEDGMENTS

We thank the ABRC for providing seeds and Barbara N. Kunkel and Chao-Ying Chen for bacteria and *B. cinerea*, respectively. We also thank the Technology Commons (TechComm), College of Life Science, National Taiwan University for providing RT-qPCR equipment. We appreciate the help of Yi-Fang Tsay (Academia Sinica, Taiwan) in providing technical and instrumental support for the oocyte patch clamp. This work was supported by the Ministry of Science and Technology of Taiwan (grants 99-2628-B-002-053-MY3, 102-2628-B-002-011-MY3, and 105-2311-B-002-032-MY3 to L.Z.) and the National Taiwan University, (Frontier and Innovative Research grant 99R70436 to L.Z.). Support was also provided by the Estonian Ministry of Science and Education (grant PRG433 to H.K.) and by the Center of Excellence in Molecular Cell Engineering (European Regional Fund).

AUTHOR CONTRIBUTIONS

C.C., D.P., and L.Z. designed the research. C.C., D.P., G.-Y.L., T.-C.C., S.Y., Y.-H.H., T.-Y.H., Y.-H.Y., and H.-L.Y. performed research. K.T. and H.K. carried out the in vitro kinase assay. E.O. and Y.M. performed the patch-clamp experiments with guard cell protoplasts. Y.-Y.W. and C.C. did the *Xenopus* oocyte patch-clamp analyses. T.-J.C. contributed new reagents/analytic tools. C.C., D.P., and L.Z. analyzed data, and C.C., D.P., and L.Z. wrote the article.

Received August 6, 2019; revised March 30, 2020; accepted April 19, 2020; published April 23, 2020.

REFERENCES

Alonso, J.M., et al. (2003). Genome-wide insertional mutagenesis of *Arabidopsis thaliana*. Science **301:** 653–657.

Antolín-Llovera, M., Ried, M.K., and Parniske, M. (2014). Cleavage of the SYMBIOSIS RECEPTOR-LIKE KINASE ectodomain promotes complex formation with Nod factor receptor 5. Curr. Biol. **24:** 422–427.

Arnaud, D., and Hwang, I. (2015). A sophisticated network of signaling pathways regulates stomatal defenses to bacterial pathogens. Mol. Plant **8:** 566–581.

Boller, T., and Felix, G. (2009). A renaissance of elicitors: Perception of microbe-associated molecular patterns and danger signals by pattern-recognition receptors. Annu. Rev. Plant Biol. **60:** 379–406.

Boudsocq, M., Willmann, M.R., McCormack, M., Lee, H., Shan, L., He, P., Bush, J., Cheng, S.H., and Sheen, J. (2010). Differential innate immune signalling via Ca(2+) sensor protein kinases. Nature **464:** 418–422.

Brandt, B., Brodsky, D.E., Xue, S., Negi, J., Iba, K., Kangasjärvi, J., Ghassemian, M., Stephan, A.B., Hu, H., and Schroeder, J.I. (2012). Reconstitution of abscisic acid activation of SLAC1 anion channel by CPK6 and OST1 kinases and branched ABI1 PP2C phosphatase action. Proc. Natl. Acad. Sci. USA **109:** 10593–10598.

Chen, Y.H., Hu, L., Punta, M., Bruni, R., Hillerich, B., Kloss, B., Rost, B., Love, J., Siegelbaum, S.A., and Hendrickson, W.A. (2010). Homologue structure of the SLAC1 anion channel for closing stomata in leaves. Nature **467:** 1074–1080.

Chinchilla, D., Zipfel, C., Robatzek, S., Kemmerling, B., Nürnberger, T., Jones, J.D.G., Felix, G., and Boller, T. (2007). A flagellin-induced complex of the receptor FLS2 and BAK1 initiates plant defence. Nature **448:** 497–500.

Clough, S.J., and Bent, A.F. (1998). Floral dip: A simplified method for *Agrobacterium*-mediated transformation of *Arabidopsis thaliana*. Plant J. **16:** 735–743.

Curtis, M.D., and Grossniklaus, U. (2003). A gateway cloning vector set for high-throughput functional analysis of genes in planta. Plant Physiol. **133:** 462–469.

Cutler, S.R., Ehrhardt, D.W., Griffitts, J.S., and Somerville, C.R. (2000). Random GFP:cDNA fusions enable visualization of subcellular structures in cells of *Arabidopsis* at a high frequency. Proc. Natl. Acad. Sci. USA **97:** 3718–3723.

Dardick, C., and Ronald, P. (2006). Plant and animal pathogen recognition receptors signal through non-RD kinases. PLoS Pathog. **2:** e2.

Desclos-Theveniau, M., Arnaud, D., Huang, T.-Y., Lin, G.J.-C., Chen, W.-Y., Lin, Y.-C., and Zimmerli, L. (2012). The *Arabidopsis* lectin receptor kinase LecRK-V.5 represses stomatal immunity induced by *Pseudomonas syringae* pv. tomato DC3000. PLoS Pathog **8:** e1002513.

Dodds, P.N., and Rathjen, J.P. (2010). Plant immunity: Towards an integrated view of plant-pathogen interactions. Nat. Rev. Genet. **11:** 539–548.

Domínguez-Ferreras, A., Kiss-Papp, M., Jehle, A.K., Felix, G., and Chinchilla, D. (2015). An overdose of the Arabidopsis coreceptor BRASSINOSTEROID INSENSITIVE1-ASSOCIATED RECEPTOR KINASE1 or its ectodomain causes autoimmunity in a SUPPRESSOR OF BIR1–1-dependent manner. Plant Physiol. **168:** 1106–1121.

Geiger, D., Scherzer, S., Mumm, P., Stange, A., Marten, I., Bauer, H., Ache, P., Matschi, S., Liese, A., Al-Rasheid, K.A.S., Romeis, T., and Hedrich, R. (2009). Activity of guard cell anion channel SLAC1 is controlled by drought-stress signaling kinase-phosphatase pair. Proc. Natl. Acad. Sci. USA **106:** 21425–21430.

Girardin, S.E., Sansonetti, P.J., and Philpott, D.J. (2002). Intracellular vs extracellular recognition of pathogens—common concepts in mammals and flies. Trends Microbiol. **10:** 193–199.

Gómez-Gómez, L., and Boller, T. (2000). FLS2: An LRR receptor-like kinase involved in the perception of the bacterial elicitor flagellin in *Arabidopsis*. Mol. Cell **5:** 1003–1011.

Gómez-Gómez, L., Felix, G., and Boller, T. (1999). A single locus determines sensitivity to bacterial flagellin in *Arabidopsis thaliana*. Plant J. **18:** 277–284.

Gust, A.A., Biswas, R., Lenz, H.D., Rauhut, T., Ranf, S., Kemmerling, B., Götz, F., Glawischnig, E., Lee, J., Felix, G., and Nürnberger, T. (2007). Bacteria-derived peptidoglycans constitute pathogen-associated molecular patterns triggering innate immunity in *Arabidopsis*. J. Biol. Chem. **282:** 32338–32348.

Guzel Deger, A., Scherzer, S., Nuhkat, M., Kedzierska, J., Kollist, H., Brosché, M., Unyayar, S., Boudsocq, M., Hedrich, R., and Roelfsema, M.R.G. (2015). Guard cell SLAC1-type anion channels mediate flagellin-induced stomatal closure. New Phytol. **208:** 162–173.

Ha, Y., Shang, Y., and Nam, K.H. (2016). Brassinosteroids modulate ABA-induced stomatal closure in Arabidopsis. J. Exp. Bot. **67:** 6297–6308.

Hanks, S.K., and Hunter, T. (1995). Protein kinases 6. The eukaryotic protein kinase superfamily: Kinase (catalytic) domain structure and classification. FASEB J. **9:** 576–596.

Häweker, H., Rips, S., Koiwa, H., Salomon, S., Saijo, Y., Chinchilla, D., Robatzek, S., and von Schaewen, A. (2010). Pattern recognition receptors require N-glycosylation to mediate plant immunity. J. Biol. Chem. **285:** 4629–4636.

Heese, A., Hann, D.R., Gimenez-Ibanez, S., Jones, A.M.E., He, K., Li, J., Schroeder, J.I., Peck, S.C., and Rathjen, J.P. (2007). The receptor-like kinase SERK3/BAK1 is a central regulator of innate immunity in plants. Proc. Natl. Acad. Sci. USA **104:** 12217–12222.

Hok, S., Danchin, E.G.J., Allasia, V., Panabières, F., Attard, A., and Keller, H. (2011). An *Arabidopsis* (malectin-like) leucine-rich repeat receptor-like kinase contributes to downy mildew disease. Plant Cell Environ. **34:** 1944–1957.

Hua, D., Wang, C., He, J., Liao, H., Duan, Y., Zhu, Z., Guo, Y., Chen, Z., and Gong, Z. (2012). A plasma membrane receptor kinase, GHR1, mediates abscisic acid- and hydrogen peroxide-regulated stomatal movement in Arabidopsis. Plant Cell **24:** 2546–2561.

Huang, P.-Y., Yeh, Y.-H., Liu, A.-C., Cheng, C.-P., and Zimmerli, L. (2014). The *Arabidopsis* LecRK-VI.2 associates with the pattern-recognition receptor FLS2 and primes *Nicotiana benthamiana* pattern-triggered immunity. Plant J. **79:** 243–255.

Huang, P.Y., and Zimmerli, L. (2014). Enhancing crop innate immunity: New promising trends. Front. Plant Sci. **5:** 624.

Huang, T.Y., Desclos-Theveniau, M., Chien, C.T., and Zimmerli, L. (2013). *Arabidopsis thaliana* transgenics overexpressing IBR3 show enhanced susceptibility to the bacterium *Pseudomonas syringae*. Plant Biol (Stuttg) **15:** 832–840.

Johnson, L.N., Noble, M.E.M., and Owen, D.J. (1996). Active and inactive protein kinases: Structural basis for regulation. Cell **85:** 149–158.

Kadota, Y., Macho, A.P., and Zipfel, C. (2016). Immunoprecipitation of plasma membrane receptor-like kinases for identification of phosphorylation sites and associated proteins. Methods Mol. Biol. **1363:** 133–144.

Kadota, Y., Sklenar, J., Derbyshire, P., Stransfeld, L., Asai, S., Ntoukakis, V., Jones, J.D.G., Shirasu, K., Menke, F., Jones, A., and Zipfel, C. (2014). Direct regulation of the NADPH oxidase RBOHD by the PRR-associated kinase BIK1 during plant immunity. Mol. Cell **54:** 43–55.

Knighton, D.R., Zheng, J.H., Ten Eyck, L.F., Ashford, V.A., Xuong, N.H., Taylor, S.S., and Sowadski, J.M. (1991). Crystal structure of the catalytic subunit of cyclic adenosine monophosphate-dependent protein kinase. Science **253:** 407–414.

Kong, Q., Sun, T., Qu, N., Ma, J., Li, M., Cheng, Y.T., Zhang, Q., Wu, D., Zhang, Z., and Zhang, Y. (2016). Two redundant receptor-like cytoplasmic kinases function downstream of pattern recognition receptors to regulate activation of SA biosynthesis. Plant Physiol. **171:** 1344–1354.

Korasick, D.A., McMichael, C., Walker, K.A., Anderson, J.C., Bednarek, S.Y., and Heese, A. (2010). Novel functions of Stomatal Cytokinesis-Defective 1 (SCD1) in innate immune responses against bacteria. J. Biol. Chem. **285:** 23342–23350.

Lee, D., Bourdais, G., Yu, G., Robatzek, S., and Coaker, G. (2015). Phosphorylation of the plant immune regulator RPM1-INTERACTING PROTEIN4 enhances plant plasma membrane H^+-ATPase activity and inhibits flagellin-triggered immune responses in Arabidopsis. Plant Cell **27:** 2042–2056.

Lee, L.Y., and Gelvin, S.B. (2014). Bimolecular fluorescence complementation for imaging protein interactions in plant hosts of microbial pathogens. Methods Mol. Biol. **1197:** 185–208.

Lee, S., Choi, H., Suh, S., Doo, I.S., Oh, K.Y., Choi, E.J., Schroeder Taylor, A.T., Low, P.S., and Lee, Y. (1999). Oligogalacturonic acid and chitosan reduce stomatal aperture by inducing the evolution of reactive oxygen species from guard cells of tomato and *Commelina communis*. Plant Physiol. **121:** 147–152.

Lee, S.C., Lan, W., Buchanan, B.B., and Luan, S. (2009). A protein kinase-phosphatase pair interacts with an ion channel to regulate ABA signaling in plant guard cells. Proc. Natl. Acad. Sci. USA **106:** 21419–21424.

Leung, J., Merlot, S., and Giraudat, J. (1997). The Arabidopsis ABSCISIC ACID-INSENSITIVE2 (ABI2) and ABI1 genes encode homologous protein phosphatases 2C involved in abscisic acid signal transduction. Plant Cell **9:** 759–771.

Li, L., Li, M., Yu, L., Zhou, Z., Liang, X., Liu, Z., Cai, G., Gao, L., Zhang, X., Wang, Y., Chen, S., and Zhou, J.M. (2014). The FLS2-associated kinase BIK1 directly phosphorylates the NADPH oxidase RbohD to control plant immunity. Cell Host Microbe **15:** 329–338.

Li, X., Wang, X., Yang, Y., Li, R., He, Q., Fang, X., Luu, D.-T., Maurel, C., and Lin, J. (2011). Single-molecule analysis of PIP2;1 dynamics and partitioning reveals multiple modes of *Arabidopsis* plasma membrane aquaporin regulation. Plant Cell **23:** 3780–3797.

Liang, X., Ding, P., Lian, K., Wang, J., Ma, M., Li, L., Li, L., Li, M., Zhang, X., Chen, S., Zhang, Y., and Zhou, J.-M. (2016). *Arabidopsis* heterotrimeric G proteins regulate immunity by directly coupling to the FLS2 receptor. eLife **5:** e13568.

Lim, C.W., Baek, W., Jung, J., Kim, J.H., and Lee, S.C. (2015). Function of ABA in stomatal defense against biotic and drought stresses. Int. J. Mol. Sci. **16:** 15251–15270.

Lim, C.W., and Lee, S.C. (2015). *Arabidopsis* abscisic acid receptors play an important role in disease resistance. Plant Mol. Biol. **88:** 313–324.

Lozano-Durán, R., Bourdais, G., He, S.Y., and Robatzek, S. (2014). The bacterial effector HopM1 suppresses PAMP-triggered oxidative burst and stomatal immunity. New Phytol. **202:** 259–269.

Lu, D., Wu, S., Gao, X., Zhang, Y., Shan, L., and He, P. (2010). A receptor-like cytoplasmic kinase, BIK1, associates with a flagellin receptor complex to initiate plant innate immunity. Proc. Natl. Acad. Sci. USA **107:** 496–501.

Macho, A.P., and Zipfel, C. (2014). Plant PRRs and the activation of innate immune signaling. Mol. Cell **54:** 263–272.

Mbengue, M., Bourdais, G., Gervasi, F., Beck, M., Zhou, J., Spallek, T., Bartels, S., Boller, T., Ueda, T., Kuhn, H., and Robatzek, S. (2016). Clathrin-dependent endocytosis is required for immunity mediated by pattern recognition receptor kinases. Proc. Natl. Acad. Sci. USA **113:** 11034–11039.

Melotto, M., Underwood, W., Koczan, J., Nomura, K., and He, S.Y. (2006). Plant stomata function in innate immunity against bacterial invasion. Cell **126:** 969–980.

Monaghan, J., and Zipfel, C. (2012). Plant pattern recognition receptor complexes at the plasma membrane. Curr. Opin. Plant Biol. **15:** 349–357.

Montillet, J.-L., et al. (2013). An abscisic acid-independent oxylipin pathway controls stomatal closure and immune defense in *Arabidopsis*. PLoS Biol. **11:** e1001513.

Munemasa, S., Hauser, F., Park, J., Waadt, R., Brandt, B., and Schroeder, J.I. (2015). Mechanisms of abscisic acid-mediated control of stomatal aperture. Curr. Opin. Plant Biol. **28:** 154–162.

Murata, Y., Mori, I.C., and Munemasa, S. (2015). Diverse stomatal signaling and the signal integration mechanism. Annu. Rev. Plant Biol. **66:** 369–392.

Mustilli, A.C., Merlot, S., Vavasseur, A., Fenzi, F., and Giraudat, J. (2002). Arabidopsis OST1 protein kinase mediates the regulation of stomatal aperture by abscisic acid and acts upstream of reactive oxygen species production. Plant Cell **14:** 3089–3099.

Negi, J., Matsuda, O., Nagasawa, T., Oba, Y., Takahashi, H., Kawai-Yamada, M., Uchimiya, H., Hashimoto, M., and Iba, K. (2008). CO2 regulator SLAC1 and its homologues are essential for anion homeostasis in plant cells. Nature **452:** 483–486.

Nühse, T.S., Peck, S.C., Hirt, H., and Boller, T. (2000). Microbial elicitors induce activation and dual phosphorylation of the Arabidopsis thaliana MAPK 6. J. Biol. Chem. **275:** 7521–7526.

Pei, Z.M., Kuchitsu, K., Ward, J.M., Schwarz, M., and Schroeder, J.I. (1997). Differential abscisic acid regulation of guard cell slow anion channels in Arabidopsis wild-type and abi1 and abi2 mutants. Plant Cell **9:** 409–423.

Pei, Z.M., Murata, Y., Benning, G., Thomine, S., Klüsener, B., Allen, G.J., Grill, E., and Schroeder, J.I. (2000). Calcium channels activated by hydrogen peroxide mediate abscisic acid signalling in guard cells. Nature **406:** 731–734.

Petutschnig, E.K., Jones, A.M.E., Serazetdinova, L., Lipka, U., and Lipka, V. (2010). The lysin motif receptor-like kinase (LysM-RLK) CERK1 is a major chitin-binding protein in *Arabidopsis thaliana* and subject to chitin-induced phosphorylation. J. Biol. Chem. **285:** 28902–28911.

Postel, S., Küfner, I., Beuter, C., Mazzotta, S., Schwedt, A., Borlotti, A., Halter, T., Kemmerling, B., and Nürnberger, T. (2010). The multifunctional leucine-rich repeat receptor kinase BAK1 is implicated in *Arabidopsis* development and immunity. Eur. J. Cell Biol. **89:** 169–174.

Ranf, S., Eschen-Lippold, L., Pecher, P., Lee, J., and Scheel, D. (2011). Interplay between calcium signalling and early signalling elements during defence responses to microbe- or damage-associated molecular patterns. Plant J. **68:** 100–113.

Robatzek, S., Chinchilla, D., and Boller, T. (2006). Ligand-induced endocytosis of the pattern recognition receptor FLS2 in *Arabidopsis*. Genes Dev. **20:** 537–542.

Roux, M., Schwessinger, B., Albrecht, C., Chinchilla, D., Jones, A., Holton, N., Malinovsky, F.G., Tör, M., de Vries, S., and Zipfel, C. (2011). The Arabidopsis leucine-rich repeat receptor-like kinases BAK1/SERK3 and BKK1/SERK4 are required for innate immunity to hemibiotrophic and biotrophic pathogens. Plant Cell **23:** 2440–2455.

Rutter, B.D., Rutter, K.L., and Innes, R.W. (2017). Isolation and quantification of plant extracellular vesicles. Bio Protoc. **7:** e2533.

Schroeder, J.I., Allen, G.J., Hugouvieux, V., Kwak, J.M., and Waner, D. (2001). Guard cell signal transduction. Annu. Rev. Plant Physiol. Plant Mol. Biol. **52:** 627–658.

Schulze, B., Mentzel, T., Jehle, A.K., Mueller, K., Beeler, S., Boller, T., Felix, G., and Chinchilla, D. (2010). Rapid heteromerization and phosphorylation of ligand-activated plant transmembrane receptors and their associated kinase BAK1. J. Biol. Chem. **285:** 9444–9451.

Schwessinger, B., Roux, M., Kadota, Y., Ntoukakis, V., Sklenar, J., Jones, A., and Zipfel, C. (2011). Phosphorylation-dependent differential regulation of plant growth, cell death, and innate immunity by the regulatory receptor-like kinase BAK1. PLoS Genet. **7:** e1002046.

Shi, H., Shen, Q., Qi, Y., Yan, H., Nie, H., Chen, Y., Zhao, T., Katagiri, F., and Tang, D. (2013). BR-SIGNALING KINASE1 physically associates with FLAGELLIN SENSING2 and regulates plant innate immunity in Arabidopsis. Plant Cell **25:** 1143–1157.

Sierla, M., Hõrak, H., Overmyer, K., Waszczak, C., Yarmolinsky, D., Maierhofer, T., Vainonen, J.P., Salojärvi, J., Denessiouk, K., Laanemets, K., Tõldsepp, K., and Vahisalu, T., et al. (2018). The receptor-like pseudokinase GHR1 is required for stomatal closure. Plant Cell **30:** 2813–2837.

Singh, P., and Zimmerli, L. (2013). Lectin receptor kinases in plant innate immunity. Front. Plant Sci. **4:** 124.

Singh, P., Kuo, Y.-C., Mishra, S., Tsai, C.-H., Chien, C.-C., Chen, C.-W., Desclos-Theveniau, M., Chu, P.-W., Schulze, B., Chinchilla, D., Boller, T., and Zimmerli, L. (2012). The lectin receptor kinase-VI.2 is required for priming and positively regulates Arabidopsis pattern-triggered immunity. Plant Cell **24:** 1256–1270.

Sirichandra, C., Gu, D., Hu, H.C., Davanture, M., Lee, S., Djaoui, M., Valot, B., Zivy, M., Leung, J., Merlot, S., and Kwak, J.M. (2009). Phosphorylation of the *Arabidopsis* AtrbohF NADPH oxidase by OST1 protein kinase. FEBS Lett. **583:** 2982–2986.

Spallek, T., Beck, M., Ben Khaled, S., Salomon, S., Bourdais, G., Schellmann, S., and Robatzek, S. (2013). ESCRT-I mediates FLS2 endosomal sorting and plant immunity. PLoS Genet. **9:** e1004035.

Sun, Y., Li, L., Macho, A.P., Han, Z., Hu, Z., Zipfel, C., Zhou, J.-M., and Chai, J. (2013). Structural basis for flg22-induced activation of the Arabidopsis FLS2-BAK1 immune complex. Science **342:** 624–628.

Tena, G., Boudsocq, M., and Sheen, J. (2011). Protein kinase signaling networks in plant innate immunity. Curr. Opin. Plant Biol. **14:** 519–529.

Tsai, C.-H., Singh, P., Chen, C.-W., Thomas, J., Weber, J., Mauch-Mani, B., and Zimmerli, L. (2011). Priming for enhanced defence responses by specific inhibition of the *Arabidopsis* response to coronatine. Plant J. **65:** 469–479.

Tsuda, K., and Katagiri, F. (2010). Comparing signaling mechanisms engaged in pattern-triggered and effector-triggered immunity. Curr. Opin. Plant Biol. **13:** 459–465.

Vahisalu, T., Kollist, H., Wang, Y.-F., Nishimura, N., Chan, W.-Y., Valerio, G., Lamminmäki, A., Brosché, M., Moldau, H., Desikan, R., Schroeder, J.I., and Kangasjärvi, J. (2008). SLAC1 is required for plant guard cell S-type anion channel function in stomatal signalling. Nature **452:** 487–491.

Vahisalu, T., et al. (2010). Ozone-triggered rapid stomatal response involves the production of reactive oxygen species, and is controlled by SLAC1 and OST1. Plant J. **62:** 442–453.

Vlad, F., Rubio, S., Rodrigues, A., Sirichandra, C., Belin, C., Robert, N., Leung, J., Rodriguez, P.L., Laurière, C., and Merlot, S. (2009). Protein phosphatases 2C regulate the activation of the Snf1-related kinase OST1 by abscisic acid in Arabidopsis. Plant Cell **21:** 3170–3184.

Walter, M., Chaban, C., Schütze, K., Batistic, O., Weckermann, K., Näke, C., Blazevic, D., Grefen, C., Schumacher, K., Oecking, C., Harter, K., and Kudla, J. (2004). Visualization of protein interactions in living plant cells using bimolecular fluorescence complementation. Plant J. **40:** 428–438.

Wang, X., Kota, U., He, K., Blackburn, K., Li, J., Goshe, M.B., Huber, S.C., and Clouse, S.D. (2008). Sequential transphosphorylation of the BRI1/BAK1 receptor kinase complex impacts early events in brassinosteroid signaling. Dev. Cell **15:** 220–235.

Winter, D., Vinegar, B., Nahal, H., Ammar, R., Wilson, G.V., and Provart, N.J. (2007). An "Electronic Fluorescent Pictograph" browser for exploring and analyzing large-scale biological data sets. PLoS One **2:** e718.

Xiao, F., He, P., Abramovitch, R.B., Dawson, J.E., Nicholson, L.K., Sheen, J., and Martin, G.B. (2007). The N-terminal region of *Pseudomonas* type III effector AvrPtoB elicits Pto-dependent immunity and has two distinct virulence determinants. Plant J. **52:** 595–614.

Yeh, Y.H., Panzeri, D., Kadota, Y., Huang, Y.C., Huang, P.Y., Tao, C.N., Roux, M., Chien, H.C., Chin, T.C., Chu, P.W., Zipfel, C., and Zimmerli, L. (2016). The Arabidopsis malectin-like/LRR-RLK IOS1 is critical for BAK1-dependent and BAK1-independent pattern-triggered immunity. Plant Cell **28:** 1701–1721.

Yekondi, S., Liang, F.C., Okuma, E., Radziejwoski, A., Mai, H.W., Swain, S., Singh, P., Gauthier, M., Chien, H.C., Murata, Y., and Zimmerli, L. (2018). Nonredundant functions of *Arabidopsis* LecRK-V.2 and LecRK-VII.1 in controlling stomatal immunity and jasmonate-mediated stomatal closure. New Phytol. **218:** 253–268.

Yoo, S.D., Cho, Y.H., and Sheen, J. (2007). *Arabidopsis* mesophyll protoplasts: a versatile cell system for transient gene expression analysis. Nat. Protoc. **2:** 1565–1572.

Yuan, N., Yuan, S., Li, Z., Zhou, M., Wu, P., Hu, Q., Mendu, V., Wang, L., and Luo, H. (2018). STRESS INDUCED FACTOR 2, a leucine-rich repeat kinase regulates basal plant pathogen defense. Plant Physiol. **176:** 3062–3080.

Zeng, W., Brutus, A., Kremer, J.M., Withers, J.C., Gao, X., Jones, A.D., and He, S.Y. (2011). A genetic screen reveals *Arabidopsis* stomatal and/or apoplastic defenses against Pseudomonas syringae pv. tomato DC3000. PLoS Pathog. **7:** e1002291.

Zeng, W., and He, S.Y. (2010). A prominent role of the flagellin receptor FLAGELLIN-SENSING2 in mediating stomatal response to *Pseudomonas syringae* pv tomato DC3000 in Arabidopsis. Plant Physiol. **153:** 1188–1198.

Zeng, W., Melotto, M., and He, S.Y. (2010). Plant stomata: A checkpoint of host immunity and pathogen virulence. Curr. Opin. Biotechnol. **21:** 599–603.

Zhang, J., et al. (2010). Receptor-like cytoplasmic kinases integrate signaling from multiple plant immune receptors and are targeted by a *Pseudomonas syringae* effector. Cell Host Microbe **7:** 290–301.

Zhang, S., and Klessig, D.F. (1998). Resistance gene N-mediated de novo synthesis and activation of a tobacco mitogen-activated protein kinase by tobacco mosaic virus infection. Proc. Natl. Acad. Sci. USA **95:** 7433–7438.

Zimmerli, L., Métraux, J.P., and Mauch-Mani, B. (2001). beta-Aminobutyric acid-induced protection of Arabidopsis against the necrotrophic fungus *Botrytis cinerea*. Plant Physiol. **126:** 517–523.